Technische Universität Braunschweig

SFB 880 Hochauftrieb künftiger Verkehrsflugzeuge

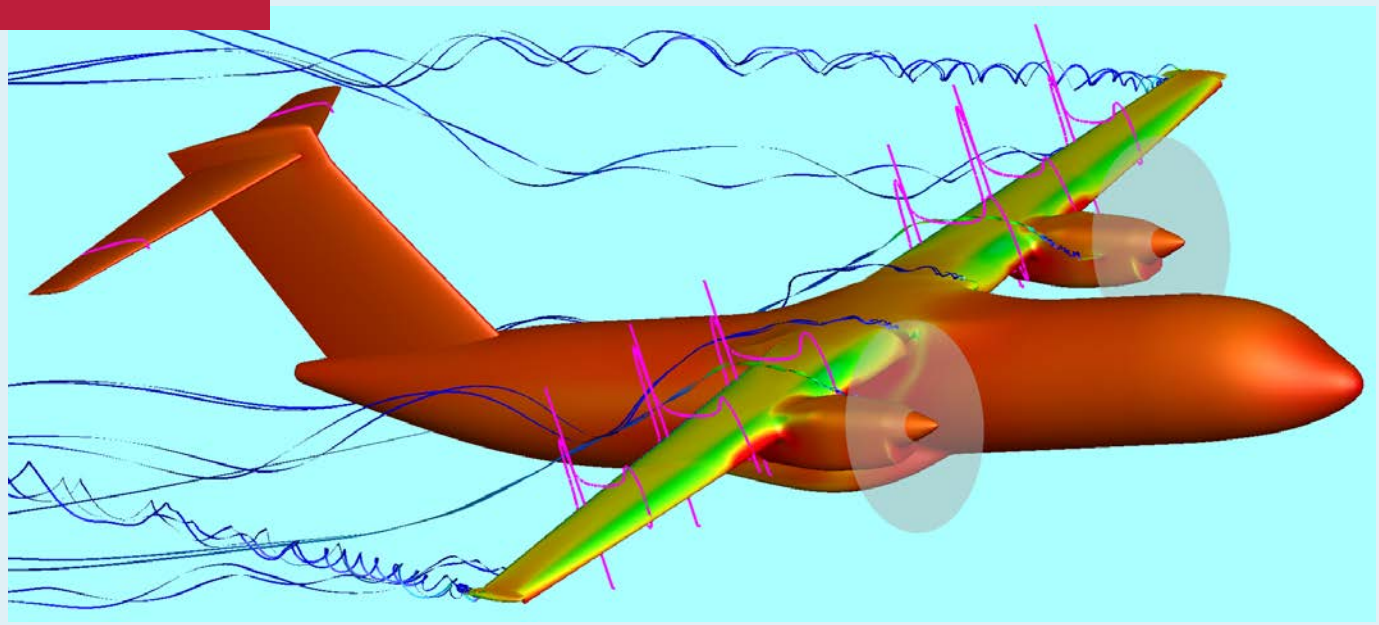

Numerical Assessment of a High-Lift Configuration with Circulation Control and flexible Droop Nose

Burnazzi Marco, Institute of Fluid Mechanics, Technische Univesität Braunschweig

Dennis Keller, Institute of Aerodynamics and Flow Technology, German Aerospace Center

December 9th 2015

DLR

Contents

- Motivation
- Introduction
- Flow mechanisms of a Coanda flap
- Design of a flexible droop nose device (2D)
- Airfoil design verification on a wing-body configuration (3D)
- Conclusion

Motivation

According to **NASA Blueprint for aeronautics** and **Vision Flightpath 2050 (ACARE)**, strategic drivers for future aviation research:

Reduction of travel time and fuel consumption are priorities to ensure sustainable air traffic growth.

Possible solution: **to extend use of existing small airports to international traffic**

- **Short runways**
- **Populated areas nearby**

New Aircraft requirements:

STOL -> effective high-lift systems
Quiet -> reduce noise sources

=> **<u>Active gap-less high-lift systems</u>**

Introduction

SFB 880: „Fundamentals of High-Lift of next generation aircraft“

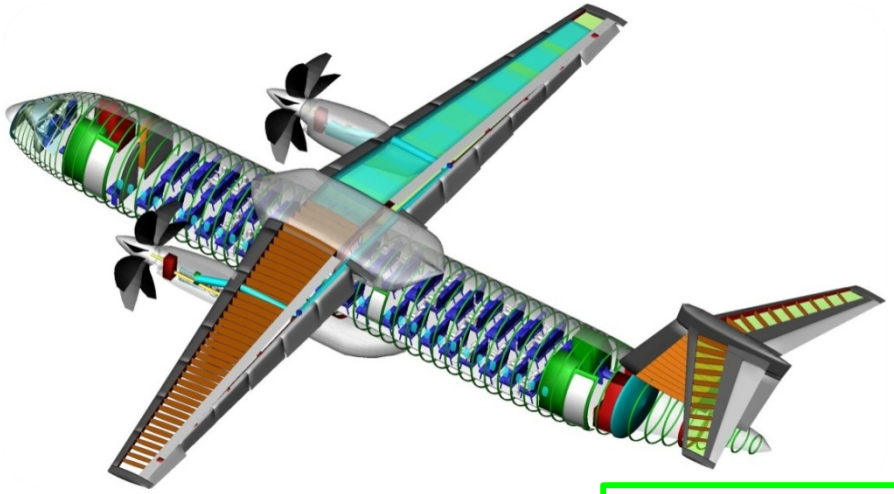

18 Subprojects:

- Lightweight Structures
- Aeroacoustics
- Aerodynamics
- Flight dynamics

Reference aircraft:

- 100 PAX
- Range: 2000 km (≈1080nm)
- MTOW : 40.641t (≈ 90000lb)
- Landing length: 800m
- **Internally Blown Flap**
- **Use of propeller slipstream**

Root Section:
F15 with increased thickness: 13.5%

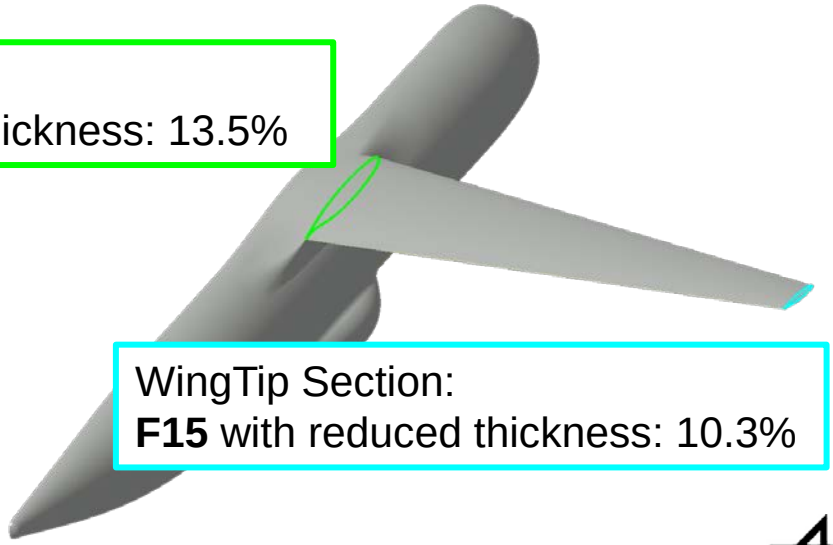

WingTip Section:
F15 with reduced thickness: 10.3%

Introduction

High-lift system

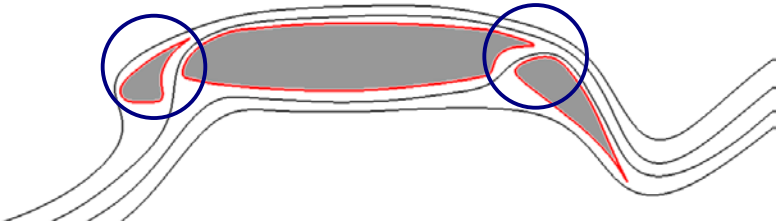

Gaps: noise and drag => Gapless active flap + droop nose

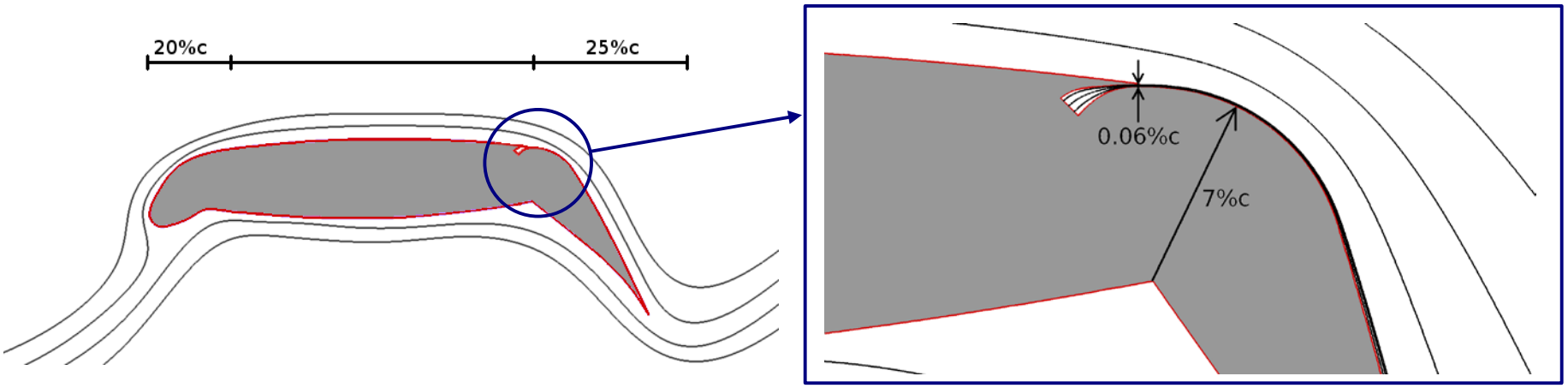

Introduction

Numerical approach

- DLR – F15 Airfoil
- DLR TAU Code
- Central scheme for the mean inviscid flow
- 2nd order Upwind Roe scheme for the convective turbulent flux
- Spalart-Allmaras turbulence model, with sarc curvature correction.
- High-density hybrid grid
- Approach validate experimentally

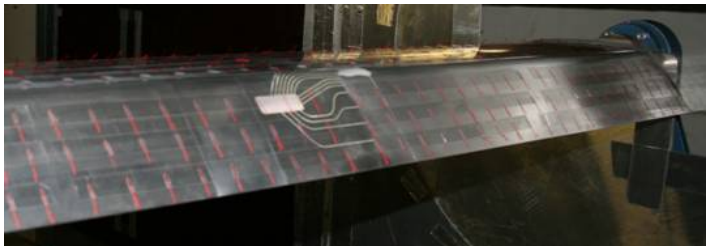

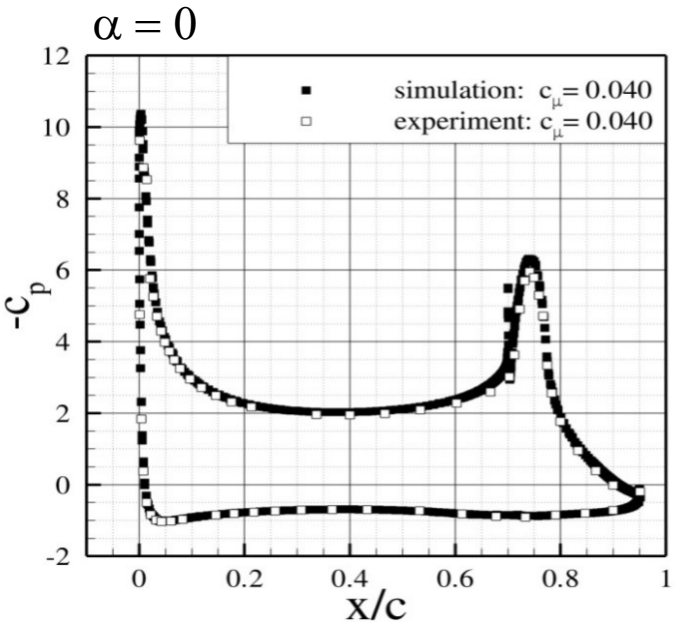

Flow mechanisms of a Coanda flap

Flow turning determined by:

- Jet momentum (C_μ)
- Angle of attack (α)
- Outer flow boundary layer (δ_2)

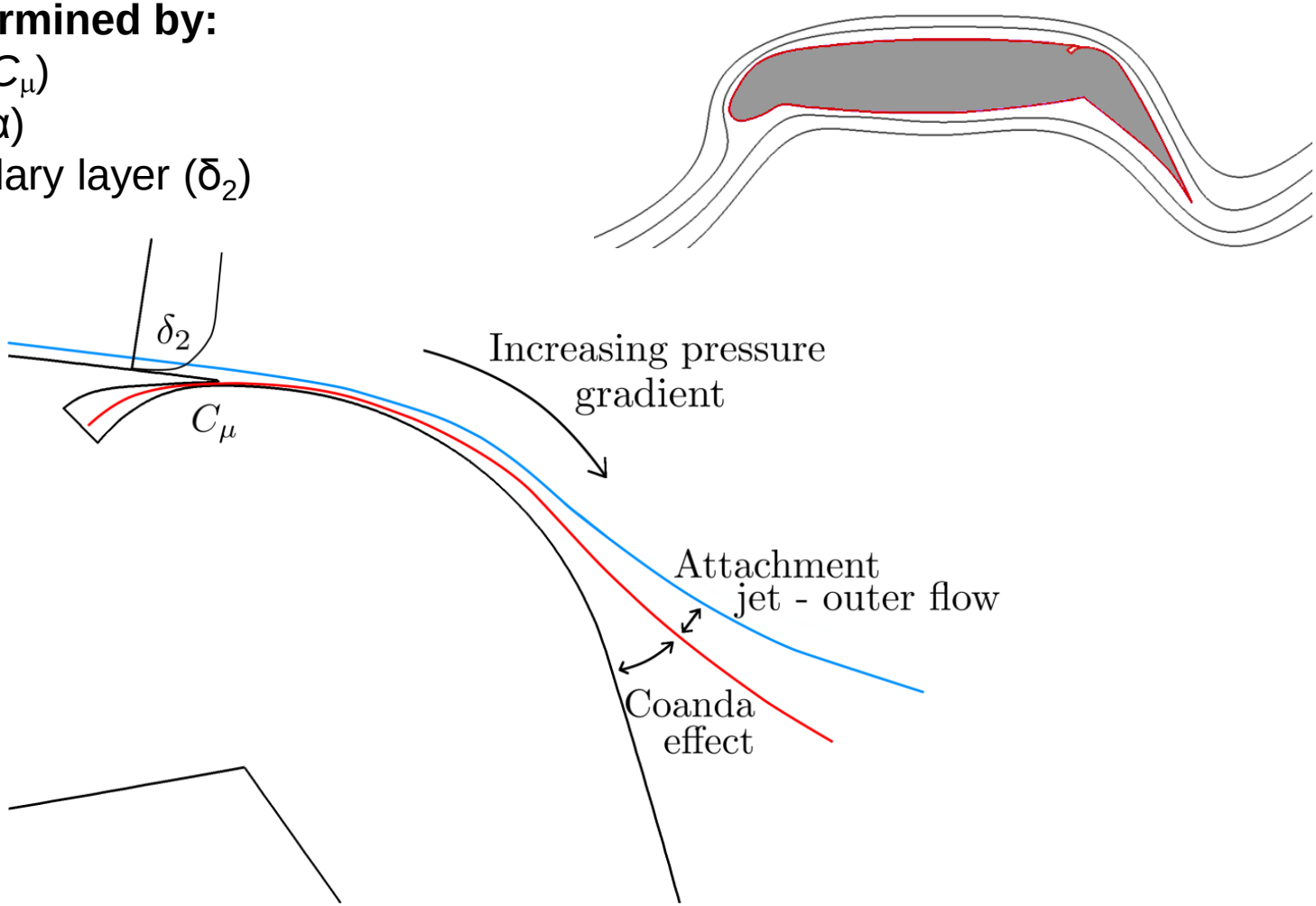

2D droop nose design

Grid

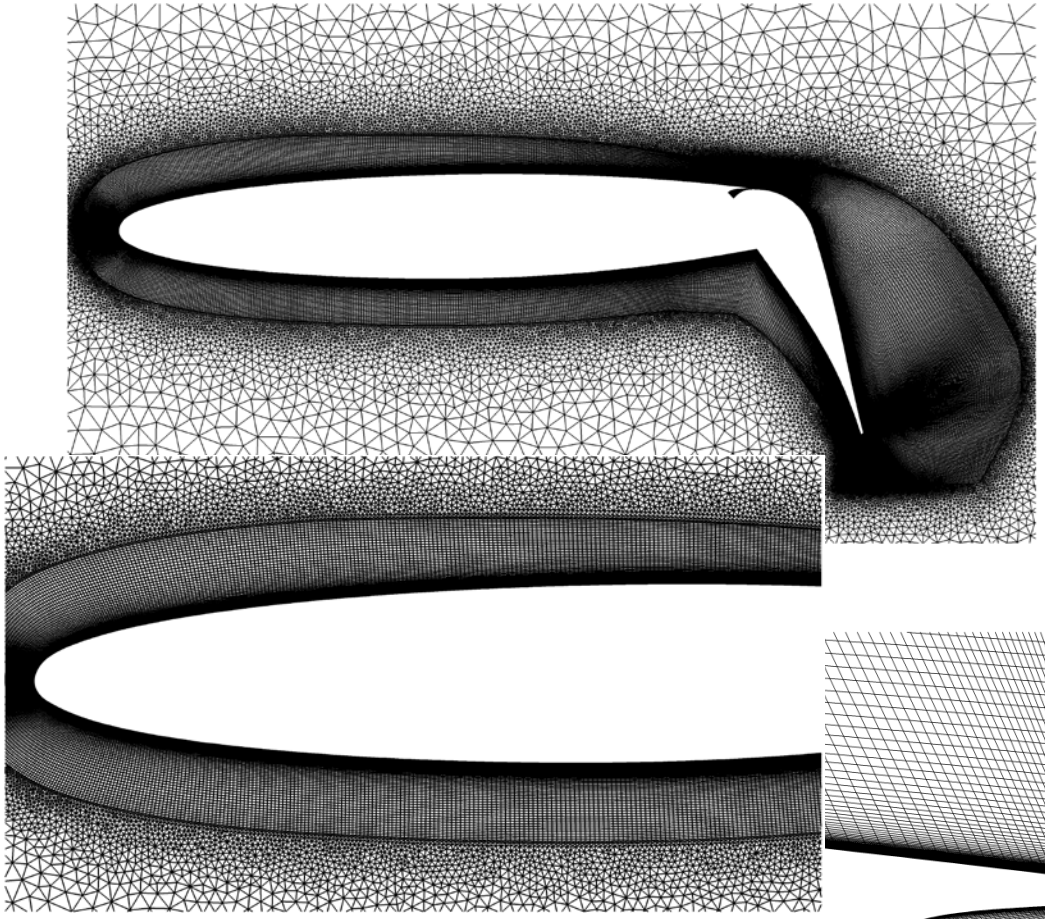

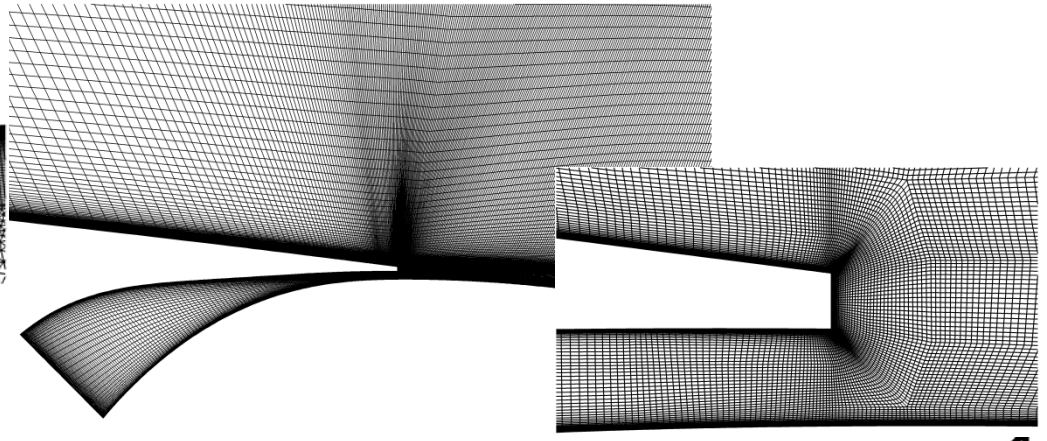

Hybrid grid

- 240000 points
- Structured mesh in ciritcal regions
- $y^+ < 1$
- High density along pressure side
- C-block topology at trailing edges

Droop nose design

Motivation

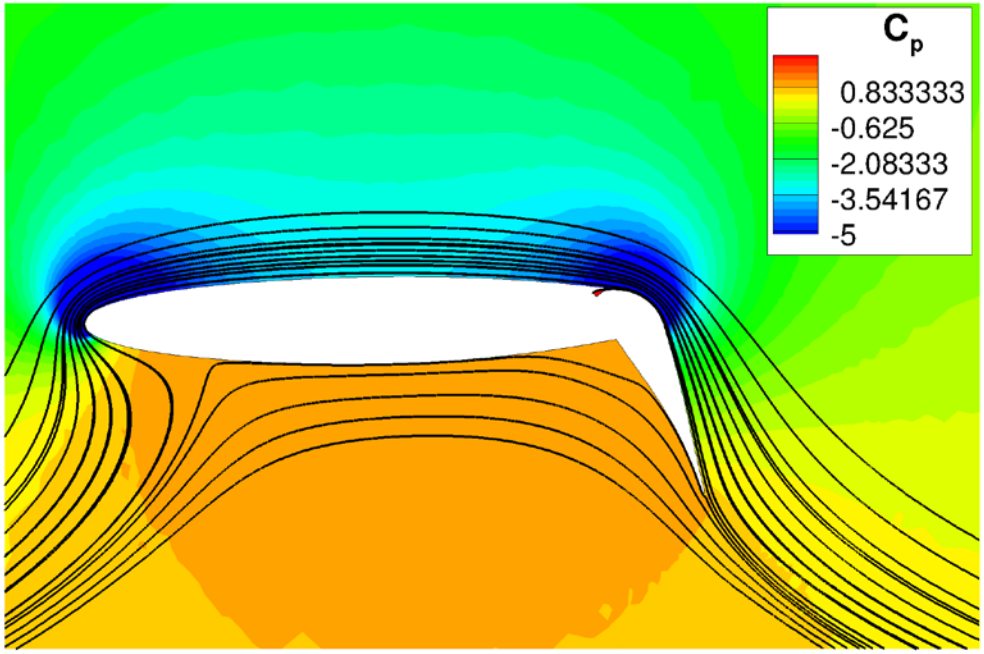

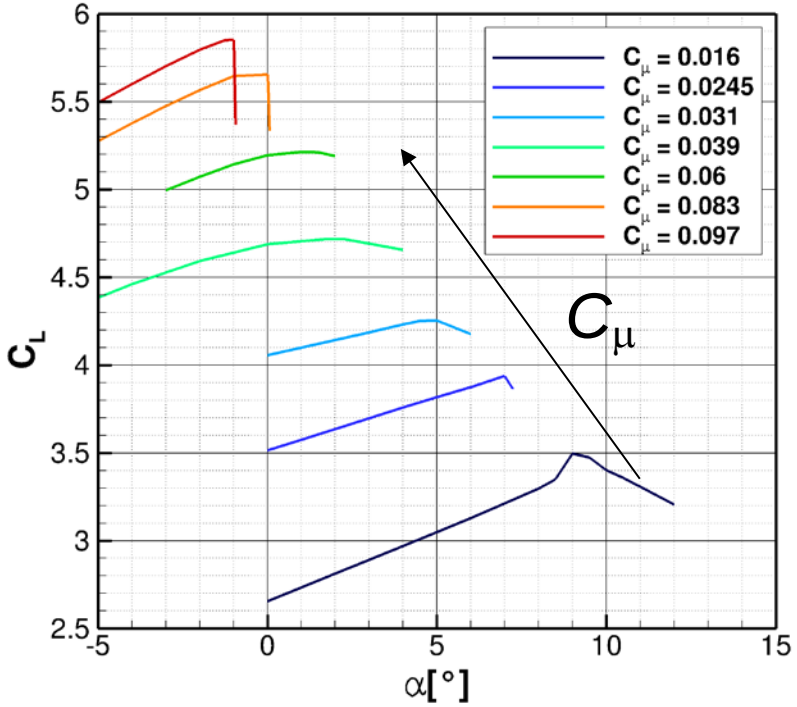

Need to increase the stall angle of attack

⇒ **Nose shape study (4 steps)**

- targets: $C_{L,max}$ and α_{stall}

- $C_\mu = 0.06$, $\delta = 65^\circ$, M = 0.15 , Re = $12 \cdot 10^6$, constant nose skin length

Droop nose design

1st step: rigid deflection of the nose

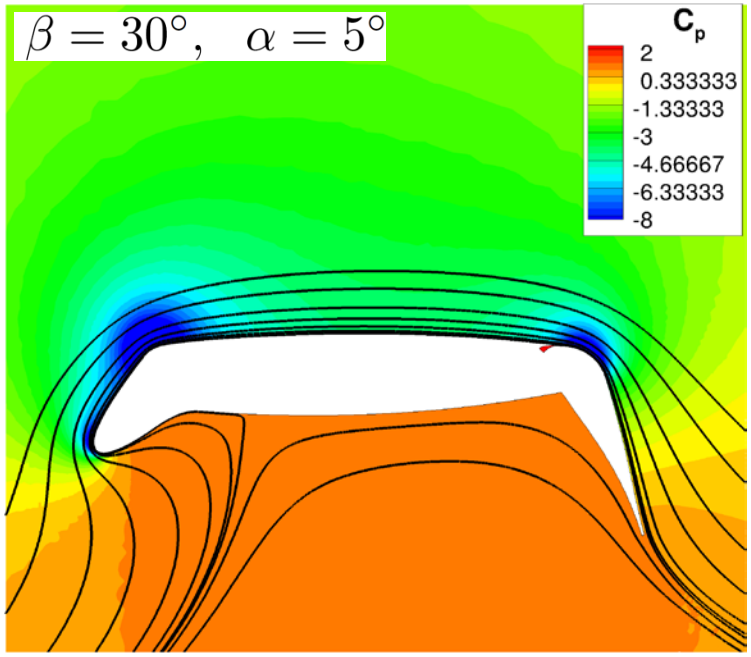

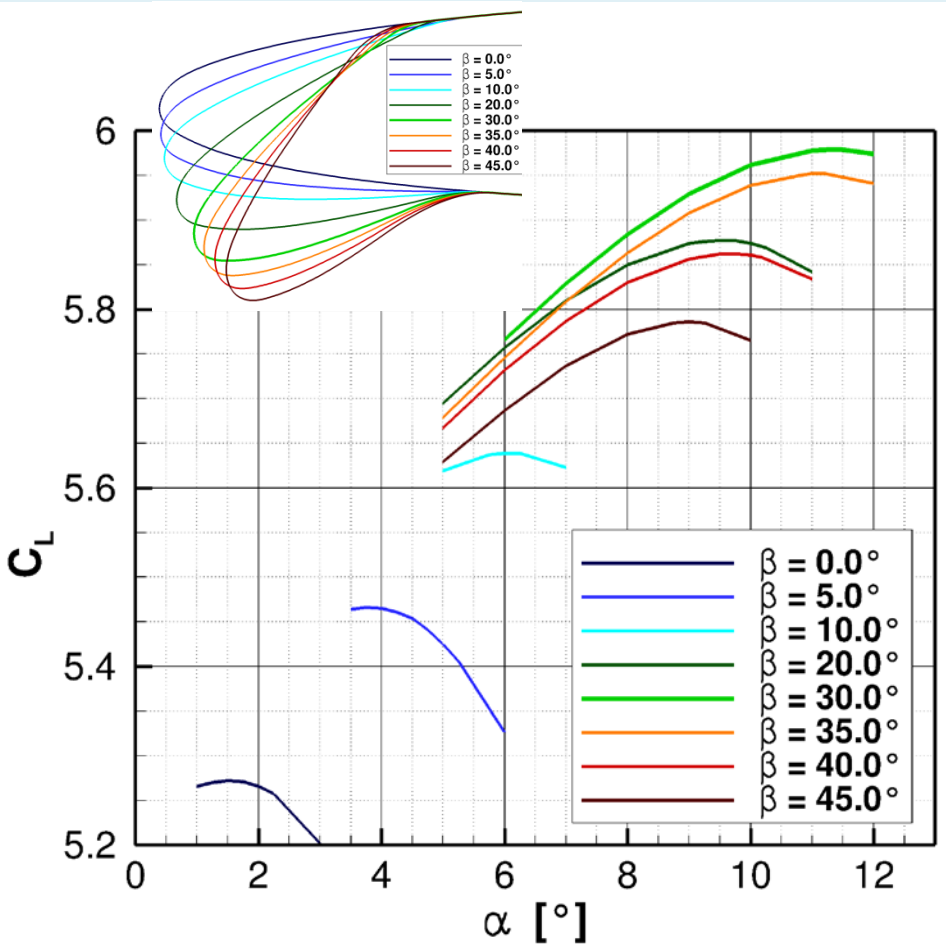

$C_{L,\,max}$: from 5.28 to 5.98 => + 13.2%

α_{stall}: from 1.5° to 11.3°

- **2 peaks of low pressure: leading edge and knee over the hinge**
- **Performance decrease with high deflection angles**

Droop nose design

2nd step: thickness increase

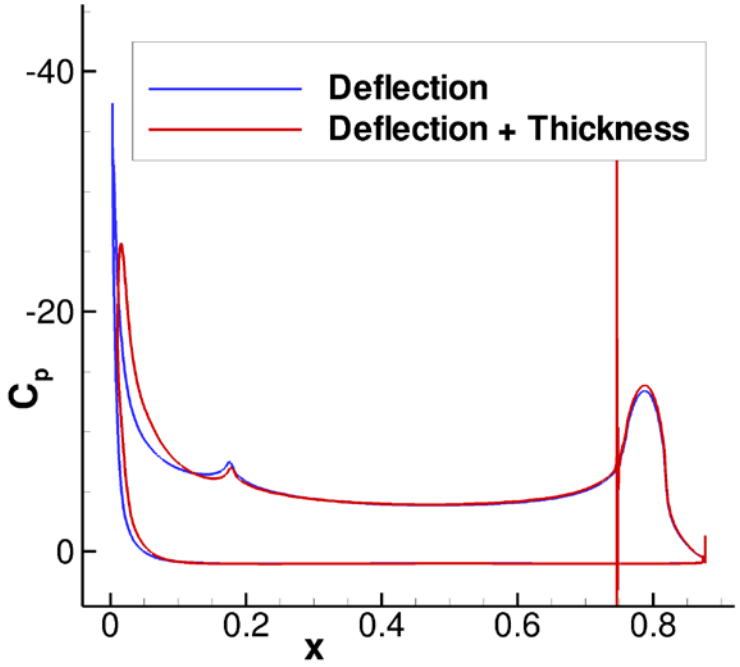

From 10° nose deflection:

$C_{L,\,max}$: from 5.64 to 5.86 => + 4 %

α_{stall} : from 6.3° to 9°

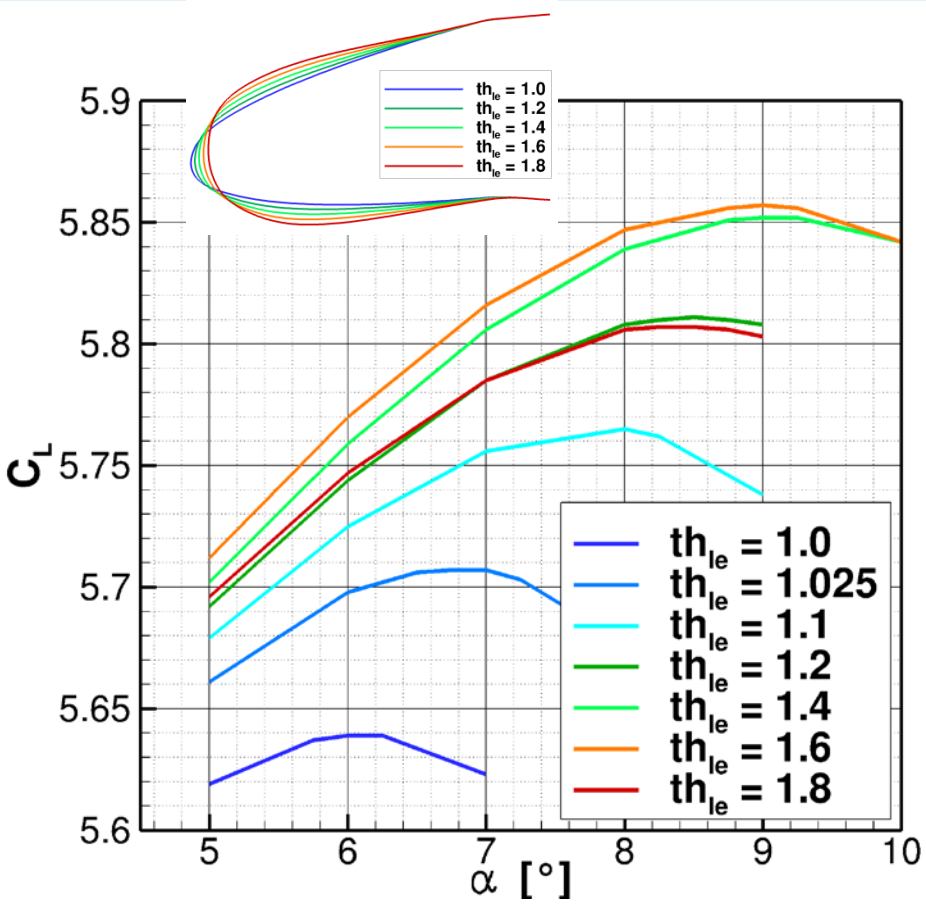

- **Improved pressure distribution on the nose**
- **Decrease of performance with high thickness**

Droop nose design

3rd step: constant camber increase

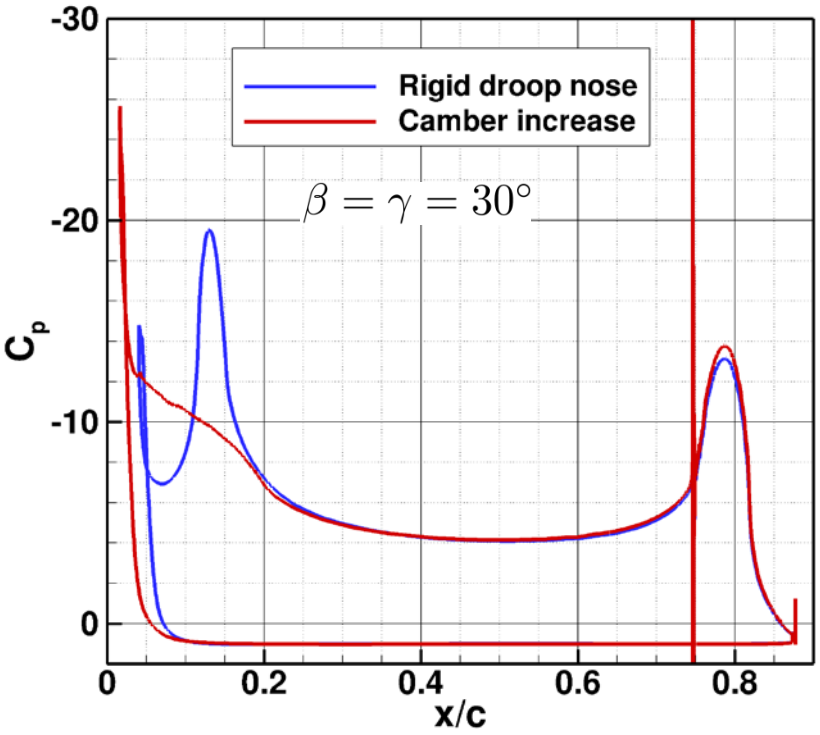

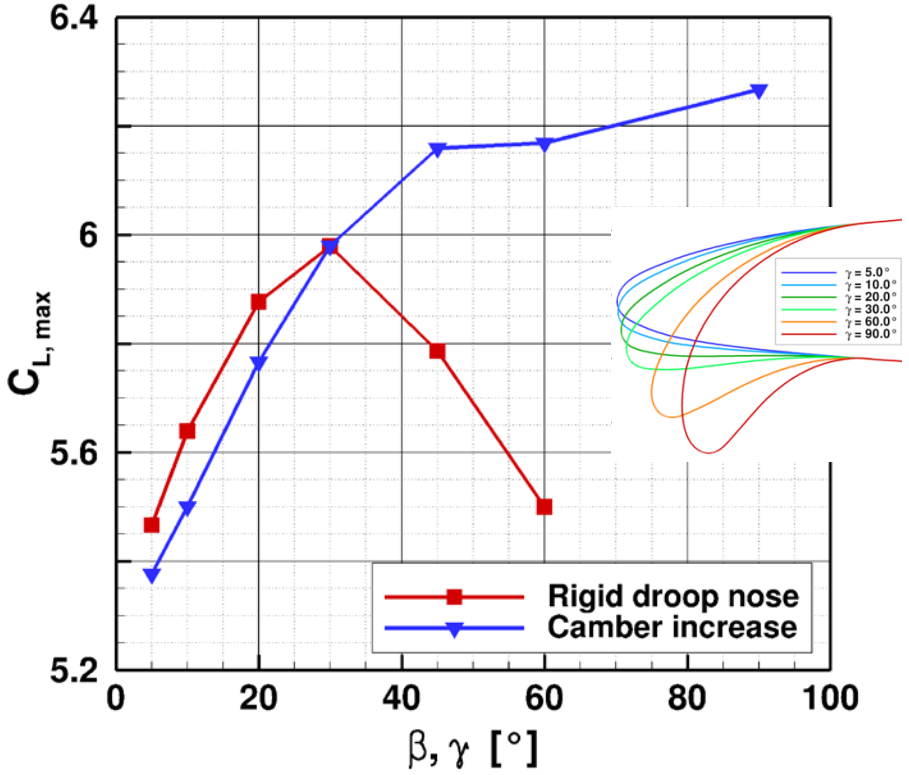

- **Further improved pressure distribution on the nose**
- **No performance decrease at high deflection angles**

$C_{L,max}$: from 5.28 to 6.19 => + 17.2%

α_{stall} : from 1.5° to 13.5°

Droop nose design

4th step: constant camber + thickness increase

Stall conditions:

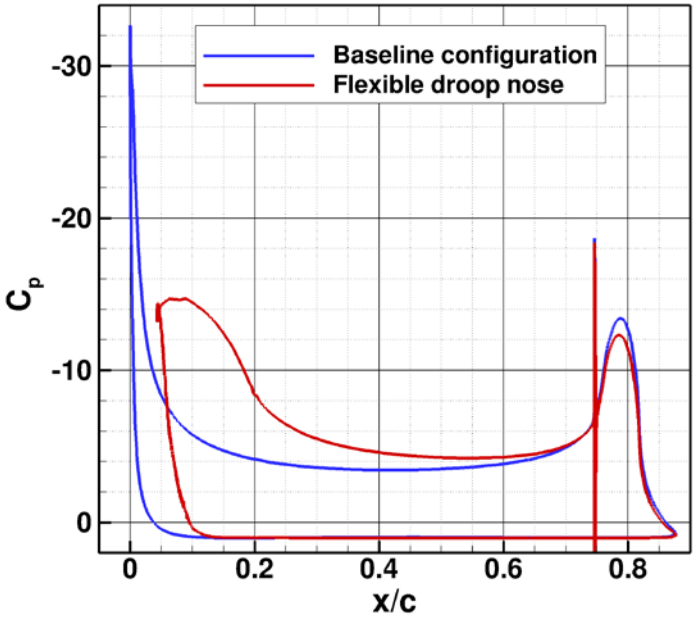

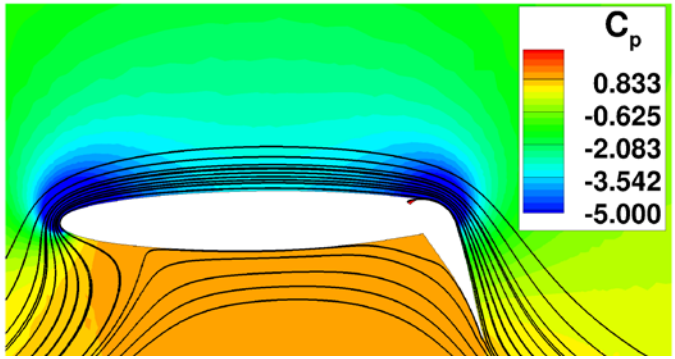

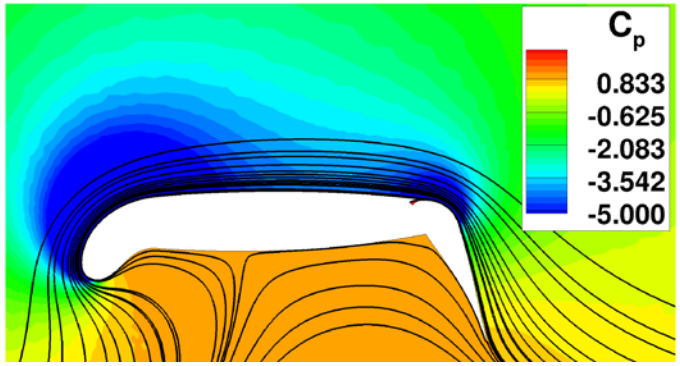

	$C_{L_{\max}}$	$\alpha_{\text{stall}}[^\circ]$	$C_{D,\text{ stall}}$	$C_{M,\text{ stall}}$
Baseline configuration	5.27	1.5	0.0886	-2.184
Camber + thickness increase	6.30	15.0	0.107	-2.44
Relative variation	+19.5%	+13.5	+20.8%	-11.7%

Droop nose performance

Droop nose effect on the Coanda flap

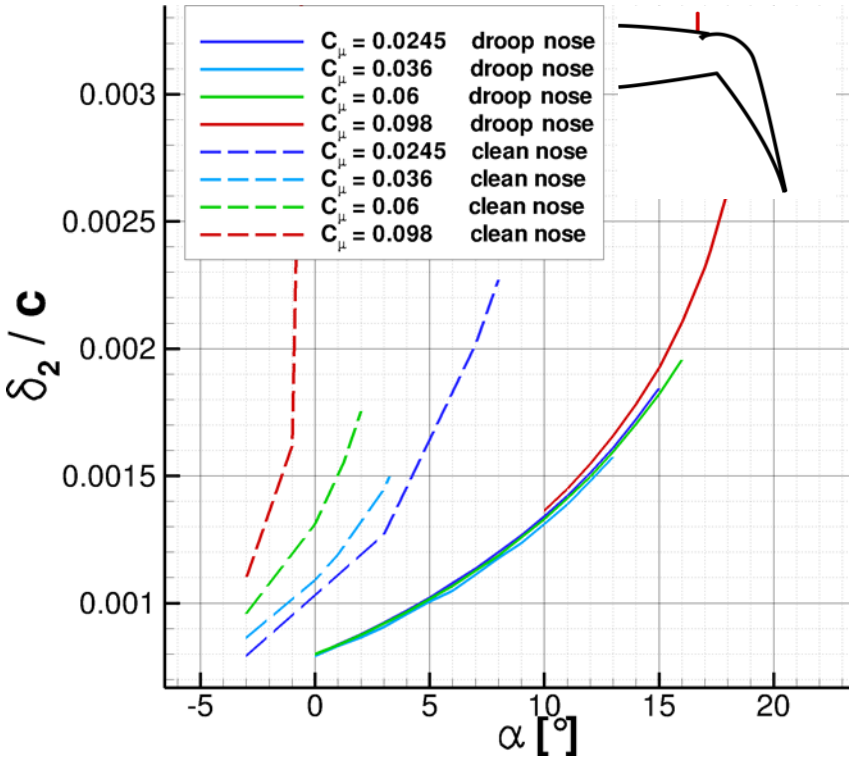

Clean nose
α = -3.0°

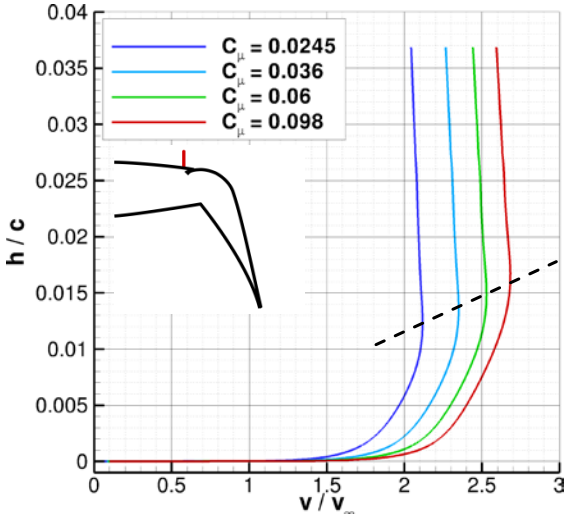

Droop nose
α = 10.0°

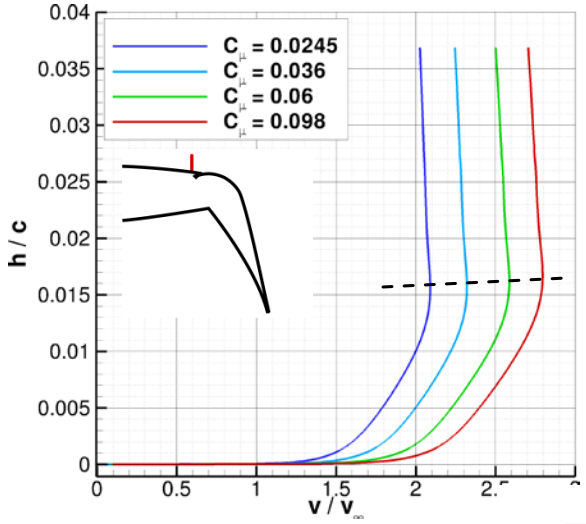

With droop nose, no significantly higher losses with C_μ

Droop nose performance

Droop nose behavior at different C_μ

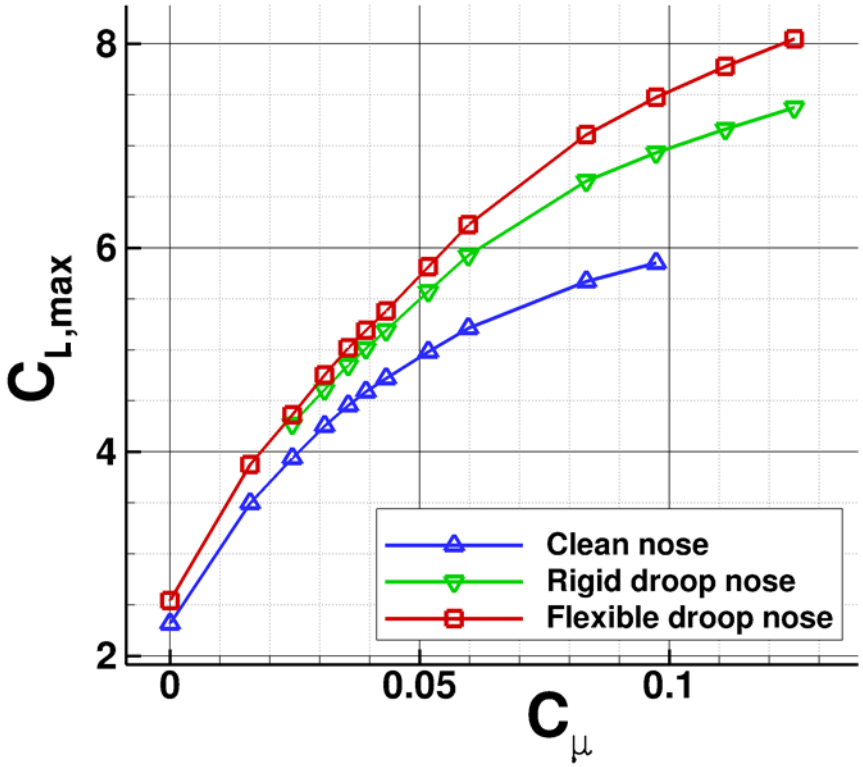

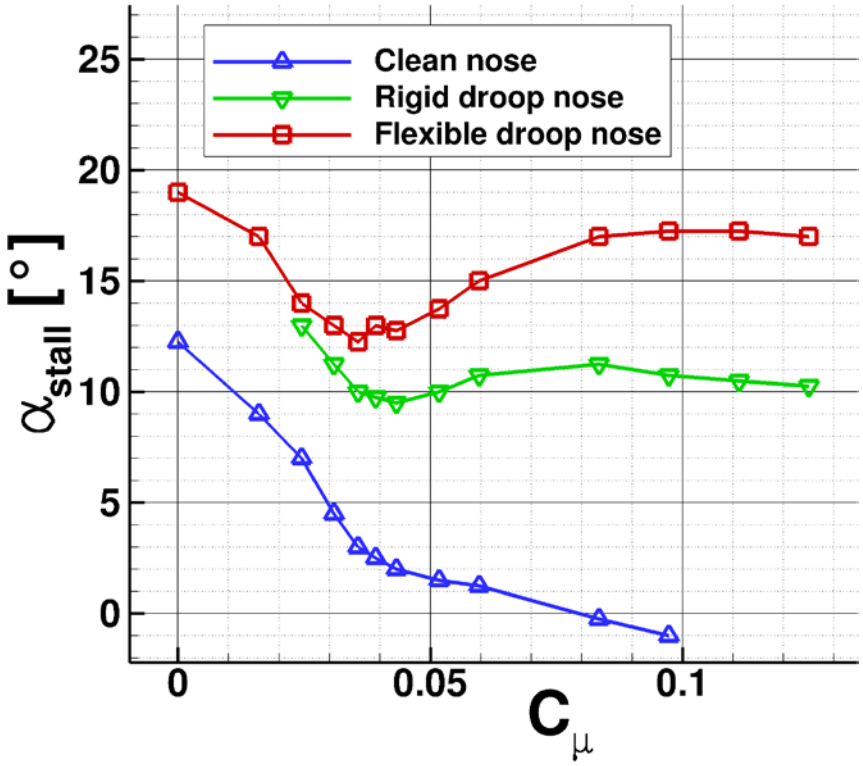

- **Leading edge device affects the reaction to different blowing rates**
- **Droop nose effect stronger for high blowing**

3D Analyses

3D Configurations/Geometry

Landing Configuration:

- Plain Flap with Circulation Control:
  - δ_{Flap}=65°, C_μ=0.036
  - $\delta_{Aileron}$=45°, C_μ=0.036
- Clean Nose or Droop Nose

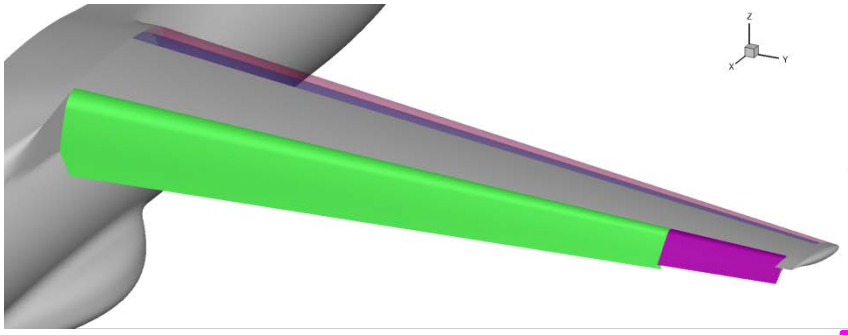

Clean Nose

Droop Nose

3D Geometry/meshing

Circulation control
- spanwise variable blowing via 6 plenum sections

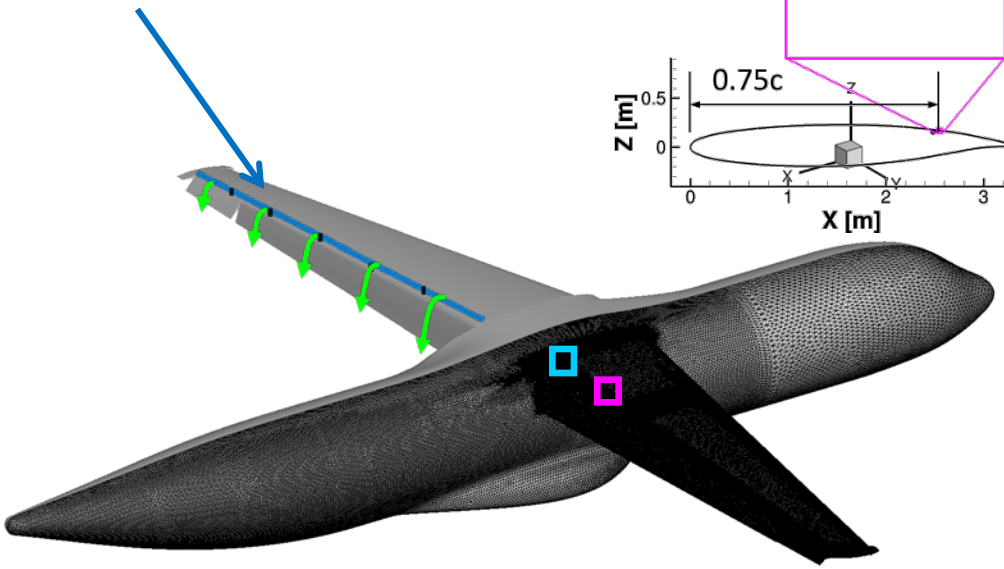

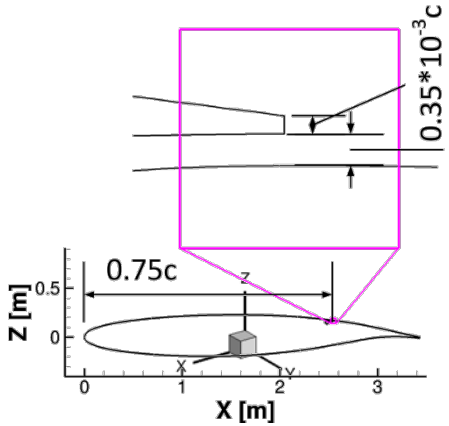

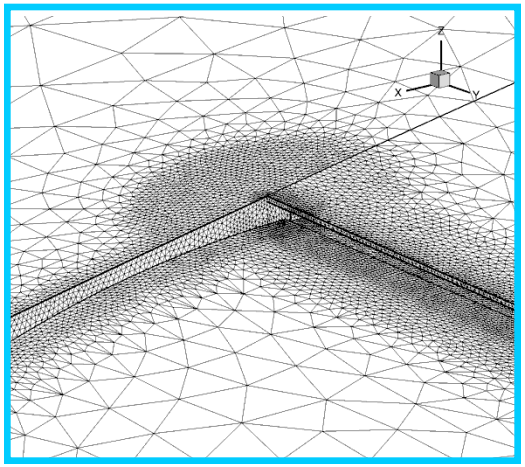

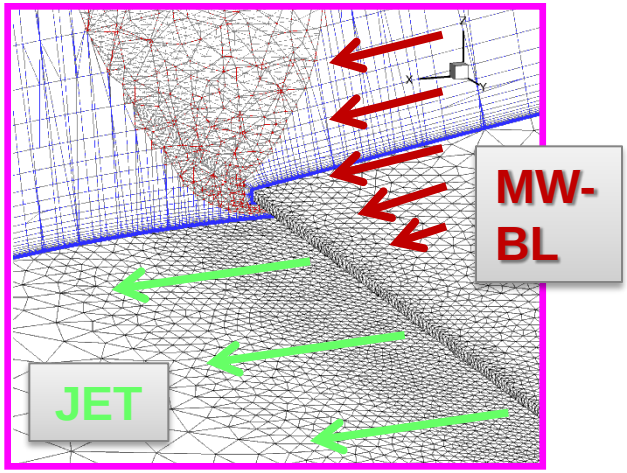

Mesh
- semi-automatic meshing w/ Centaur
- big differences in scales
- ≈40M pts (half-model)

3D Results

Alpha=6°: Overview

- Clean nose: Crossflow towards the symmetry plane
- Droop nose: Vortex directing the crossflow towards the flap

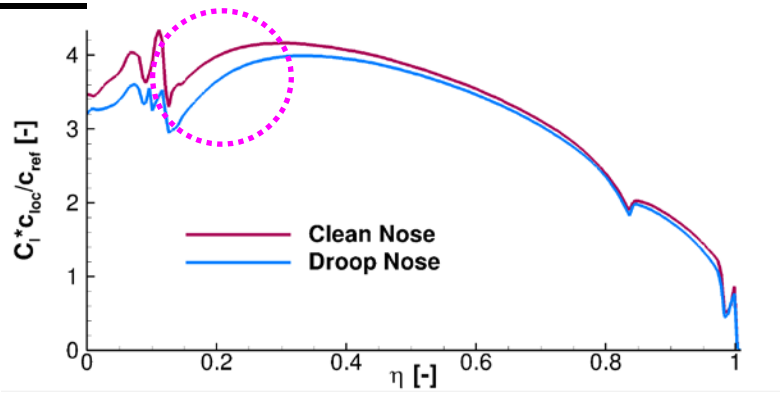

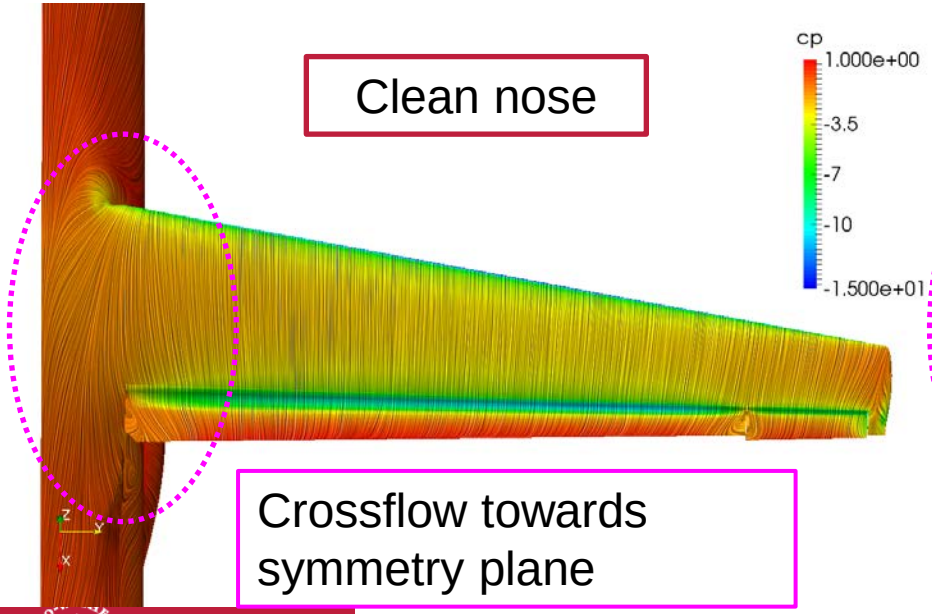

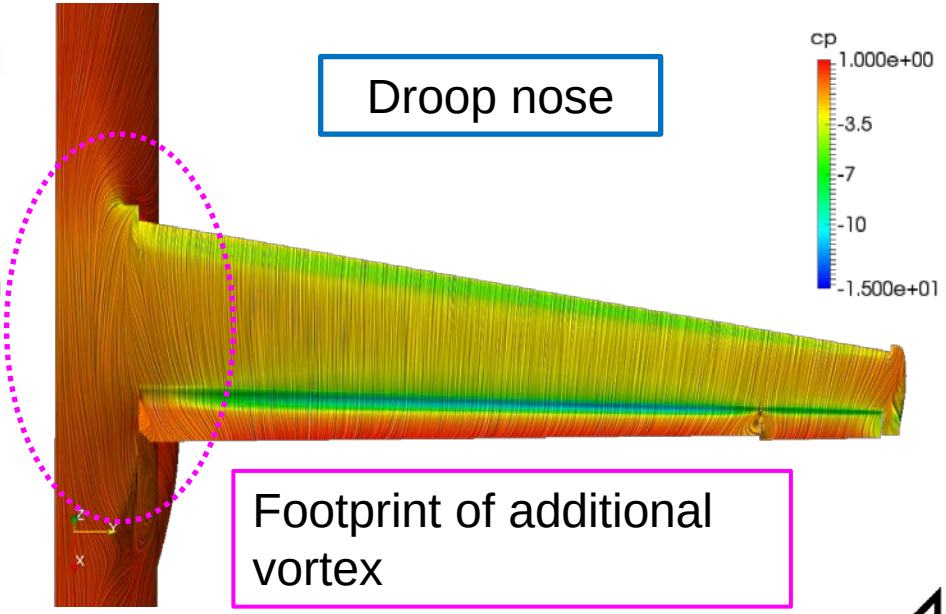

3D Results

Alpha=6°: Pressure distribution

- Strong suction peak on CN-configuration
- 0.65<η<0.7: Critical region
- Significantly reduced due to DN
- I/B flap separation larger on DN-config

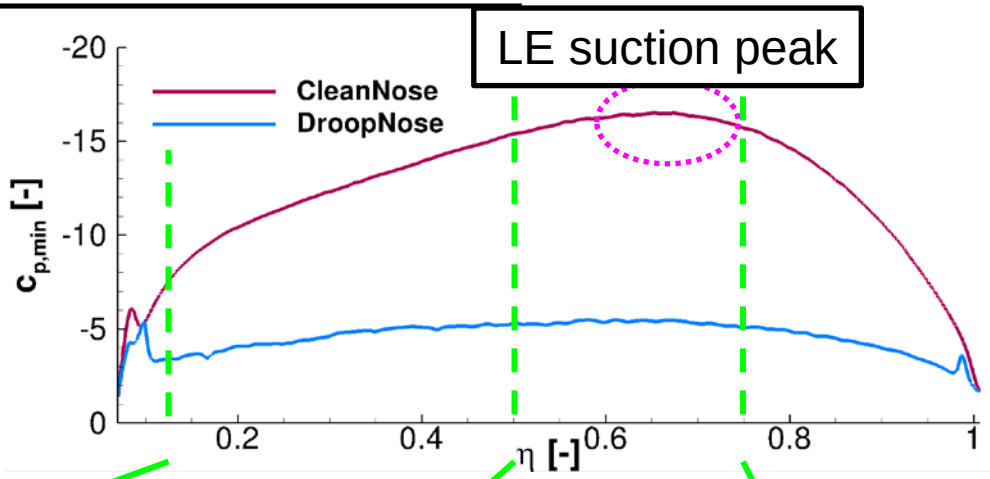

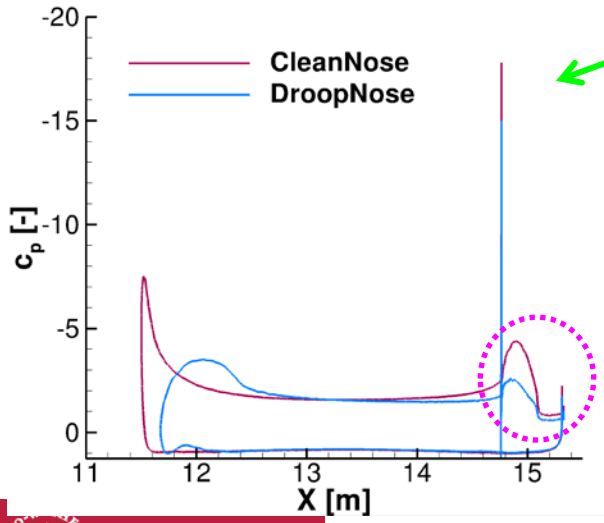

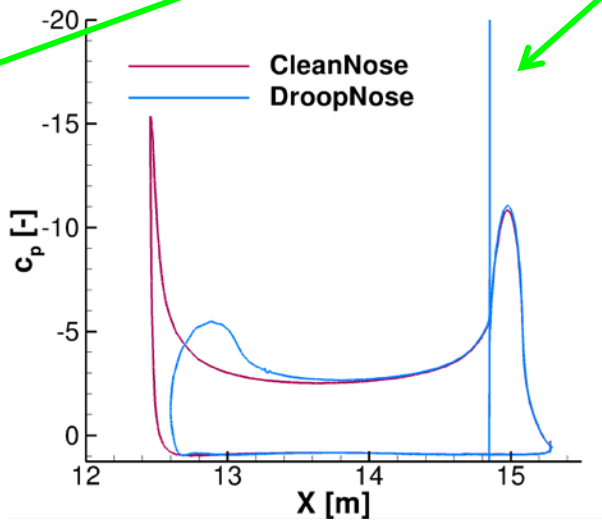

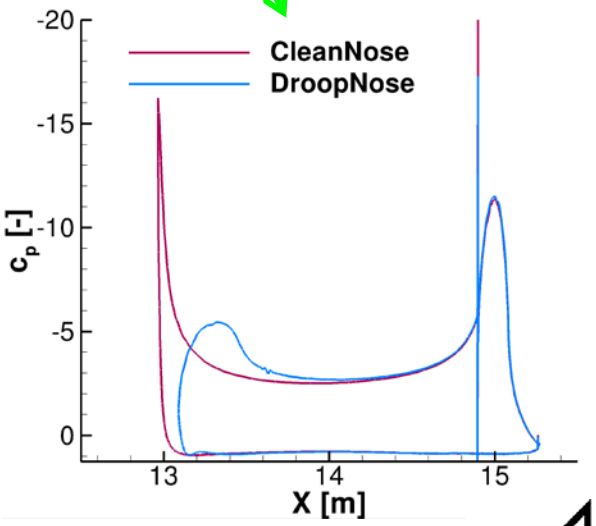

3D Results

Alpha = 12° vs 6°: Suction peak

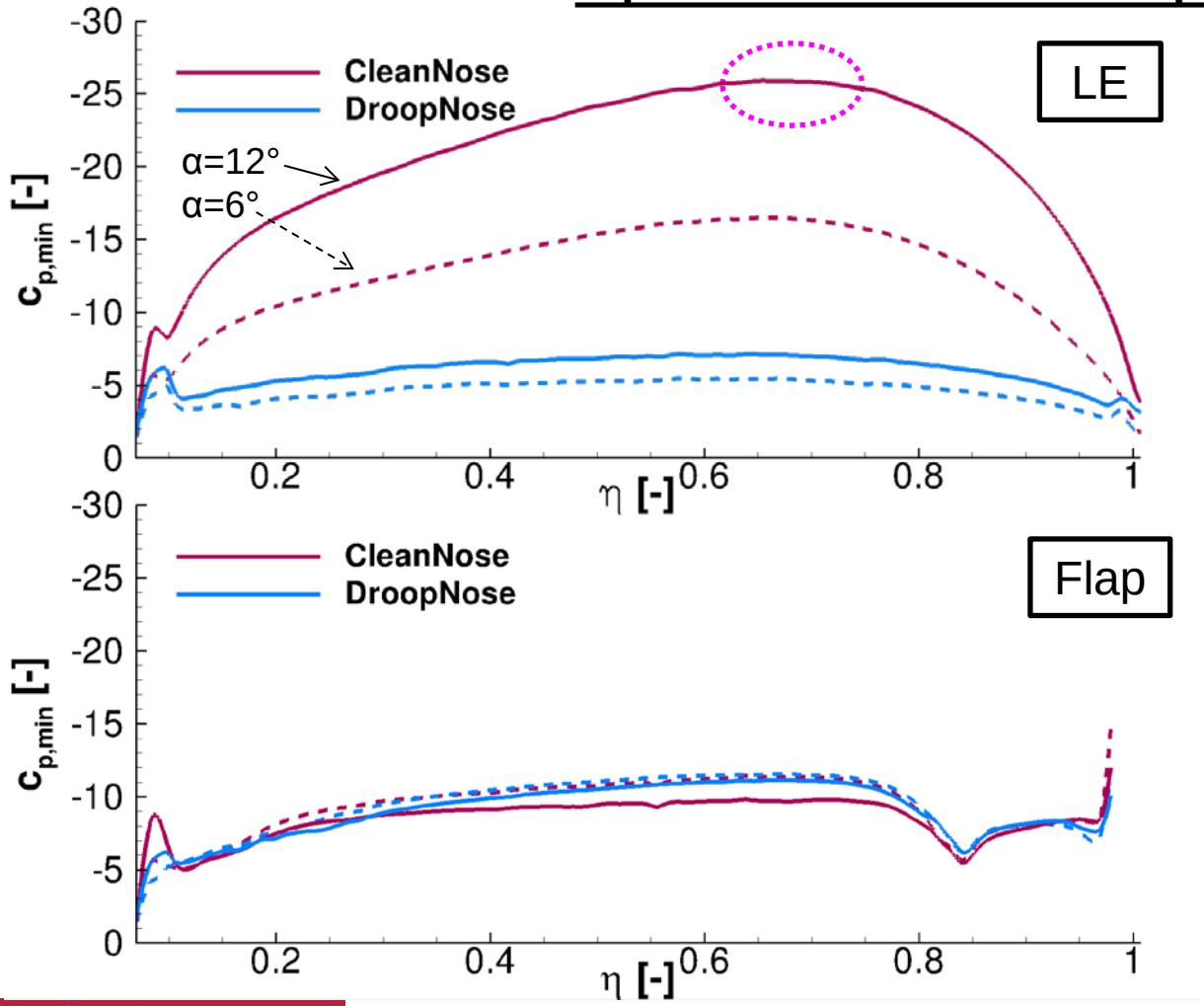

- CN:
  - Strong increase in LE suction peak
  - Reduction in Flap suction peak
- DN:
  - Slight increase in LE suction peak
  - Flap suction peak unchanged

3D Results

Alpha=6°: Inboard vortex system

Clean nose

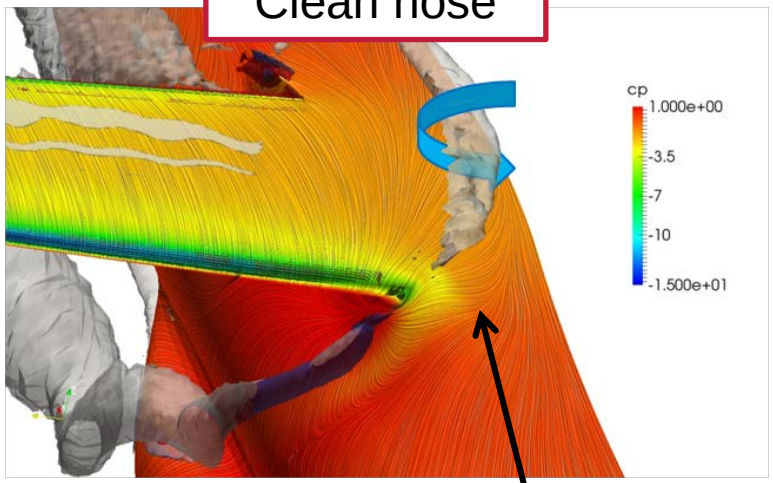

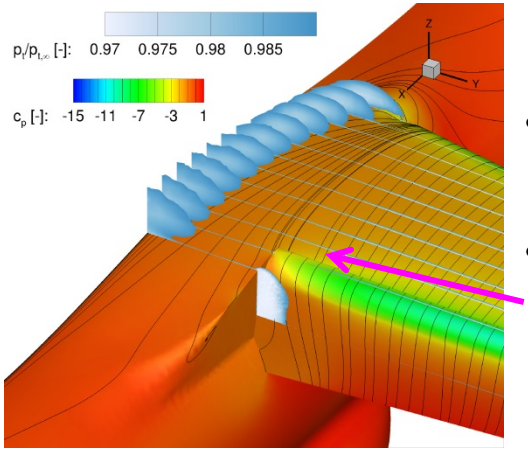

- Horseshoe vortex dominating
- „undisturbed“ m/w boundary layer at flap-body junction

Droop nose

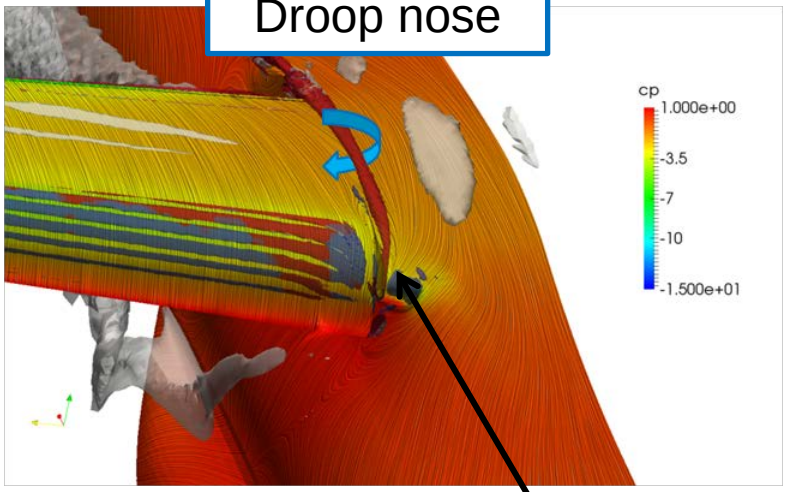

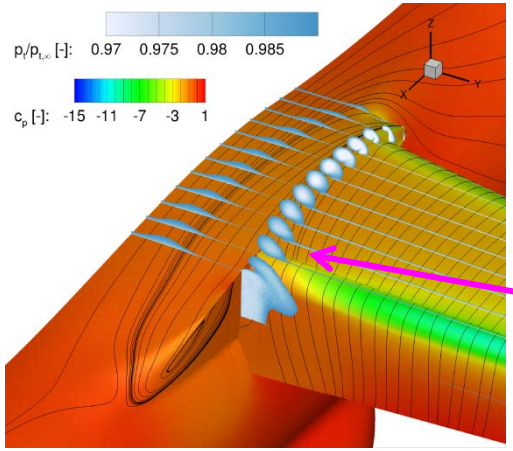

- Clean Nose side vortex dominating
- „disturbed“ m/w boundary layer at flap-body junction

3D Results

Stall mechanism

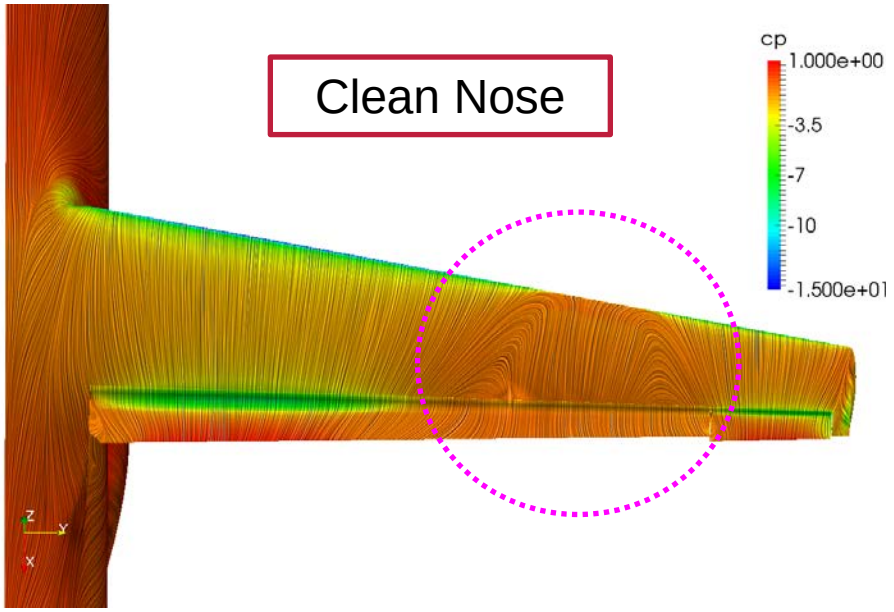

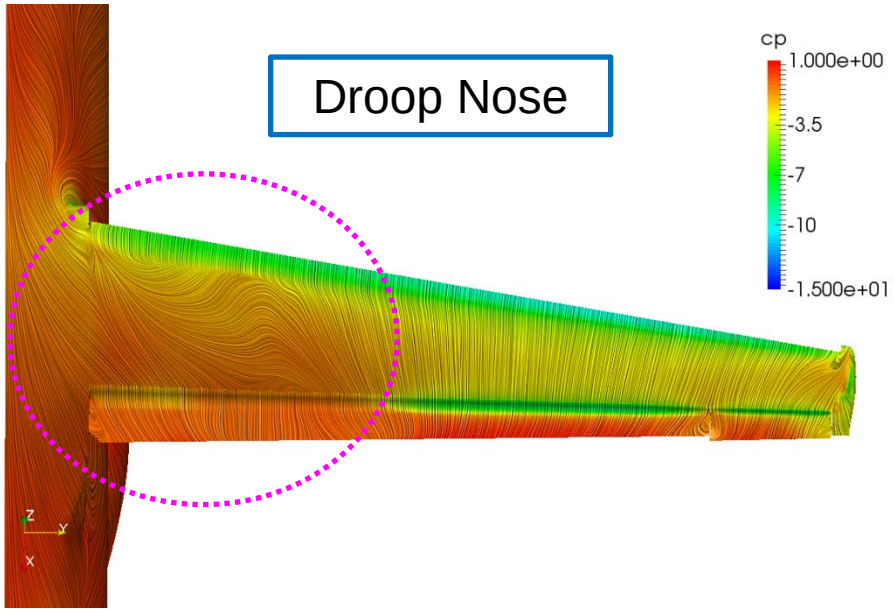

α_{stall}=12°

- Strong leading edge suction peak
  - ➢ Outboard leading edge stall

α_{stall}=22°

- Significant crossflow from the fuselage to the wing
  - ➢ Inboard trailing edge stall

3D Results

Lift Curve

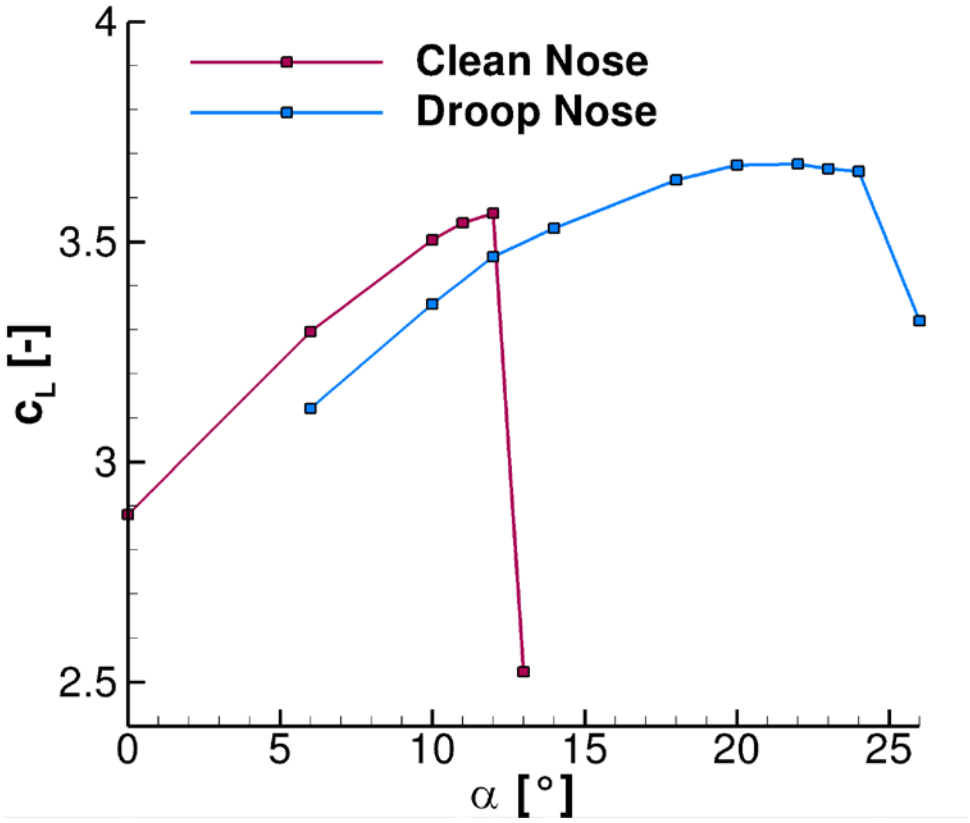

- Stall delayed by **Δα=10°**
- $c_{L,max}$ improvement by **11 lift counts**
- $c_{L,max}$ improvement limited by wing-body-junction flow

Conclusions

2D

- Aerodynamic sensitivity study of nose-shape geometrical parameters
- Analysis of the interactions among the fundamental quantities of a Coanda flap
- Maximum angle of attack delayed by **Δα=9.25°** (C_μ=0.036)
- $c_{L,max}$ improvement by **56 lift counts** (C_μ=0.036)

3D

- Integration/simulation of the optimized flexible droop nose geometry on a wing-body configuration
- Leading Edge Stall surpressed
- Inboard stall due to crossflow at wing-body junction
- Maximum angle of attack delayed by **Δα=10°** (C_μ=0.036)
- $c_{L,max}$ improvement by **11 lift counts** (C_μ=0.036)
- $c_{L,max}$ improvement limited by wing-body-junction flow

Outlook

- Experimental validation of the numerical approach and the observed 2D stall mechanisms
- Investigations of the high-lift configuration on a complete configuration (engines and tail planes)

Thank you for

your attention!

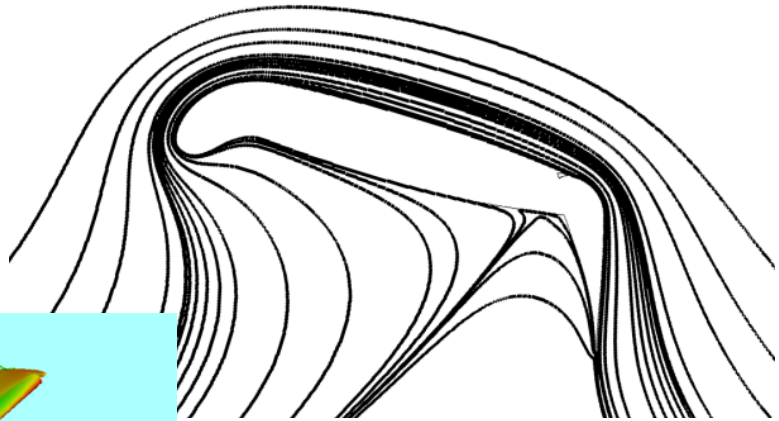

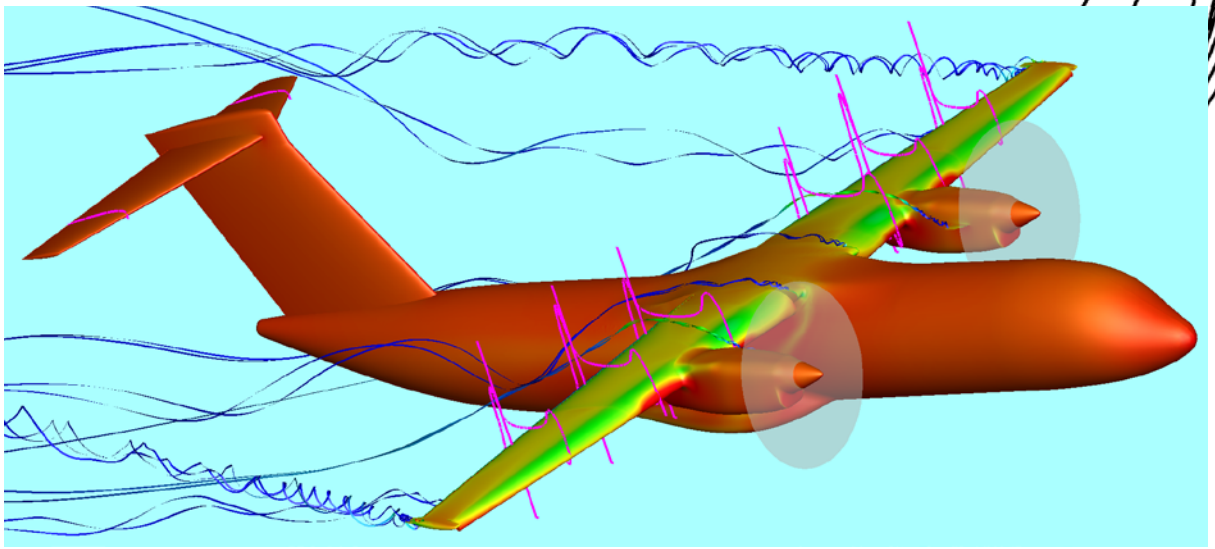

2D stall mechanism

α effect on lift generation

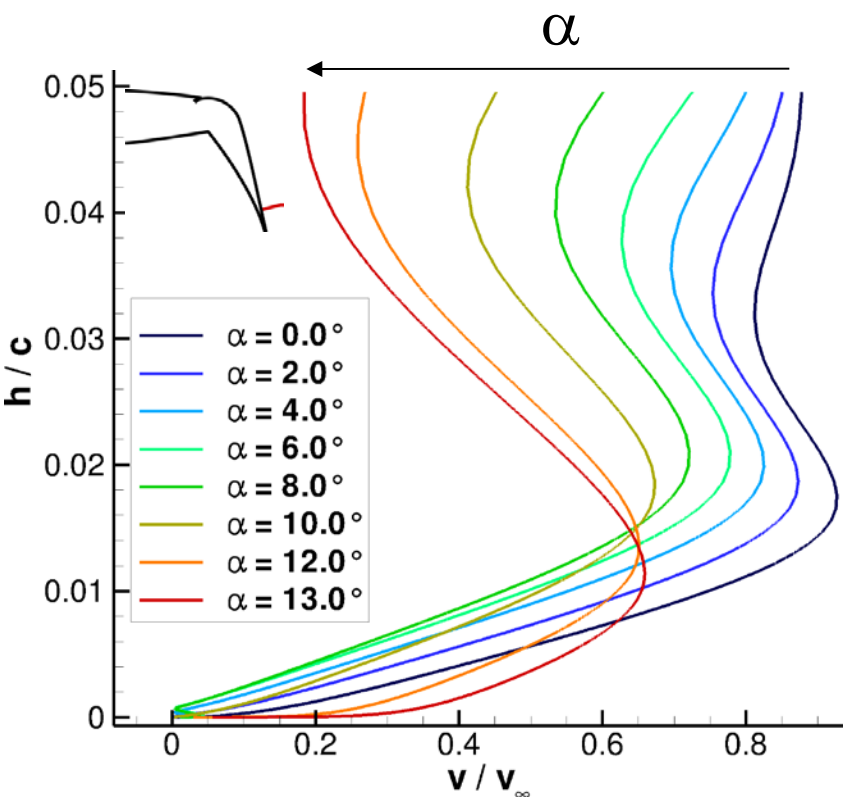

C_μ = 0.035

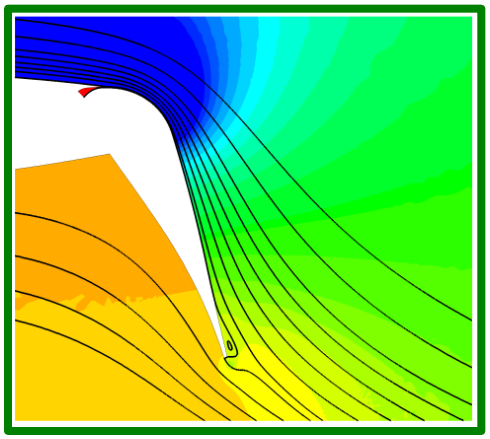

α = 8.0°

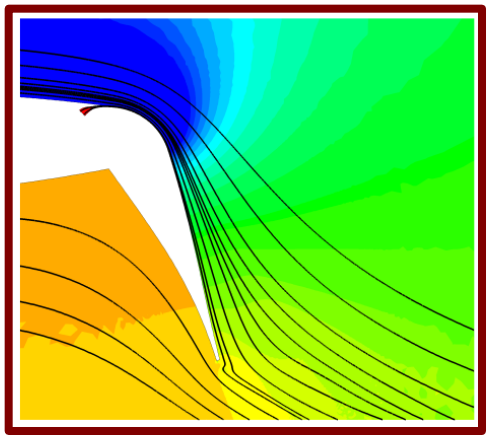

α = 13.0°

- At low α: Larger jet separation from the wall
- Gradual separation between jet and outer flow
- At high α: reattachment to the flap surface

Stall behavior of a Coanda flap

Stall behavior of the clean configuration

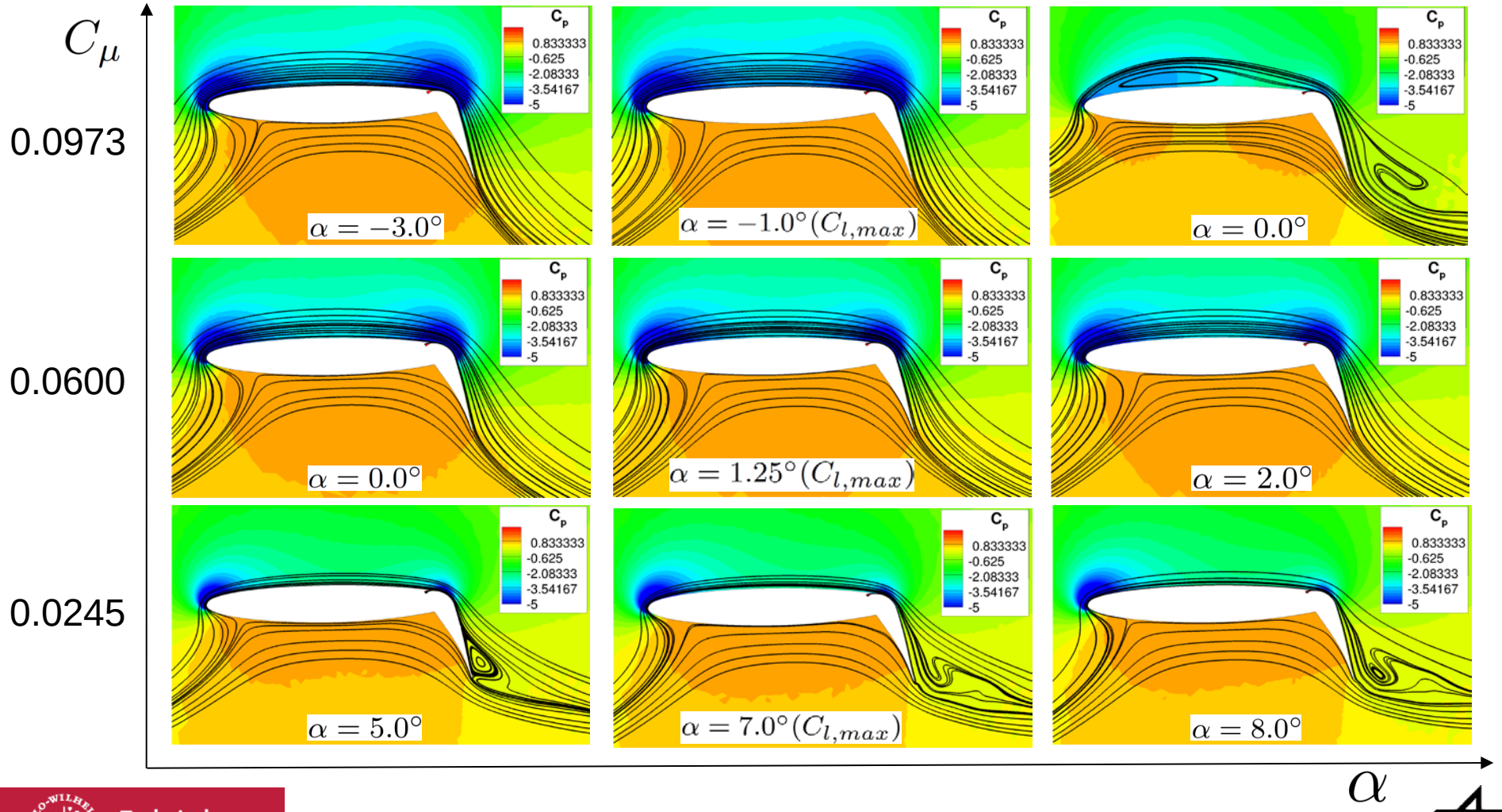

Stall behavior of a Coanda flap

Stall behavior of the droopnose configuration

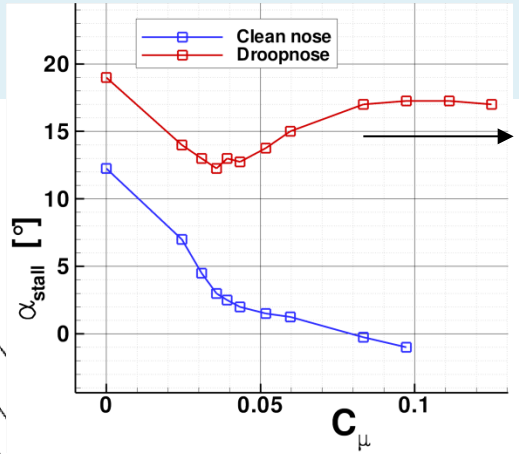

Stall behavior of a Coanda flap

Leading-edge device comparison

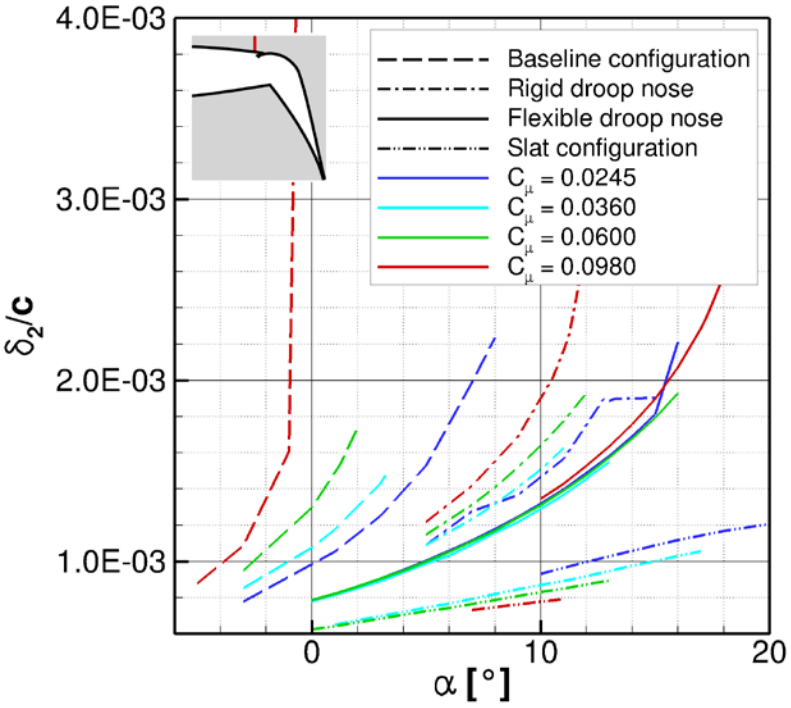

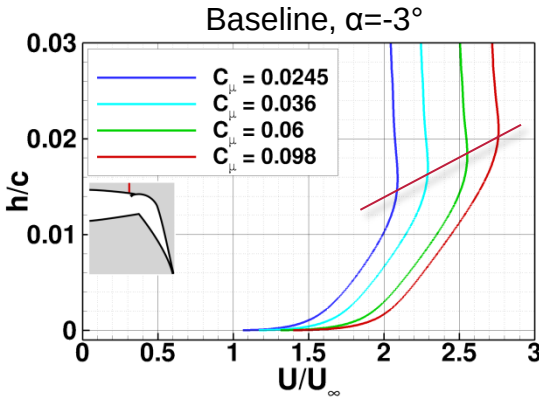

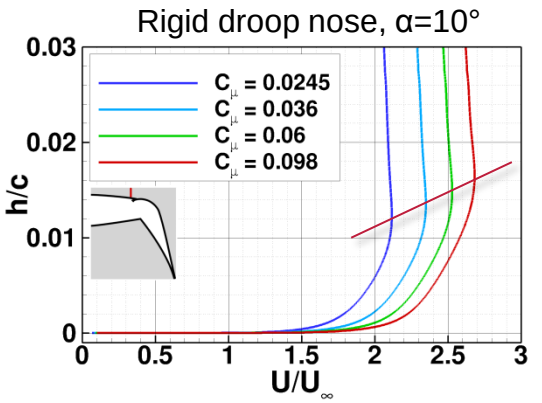

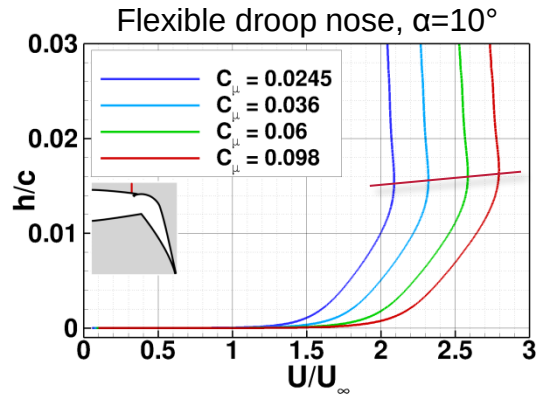

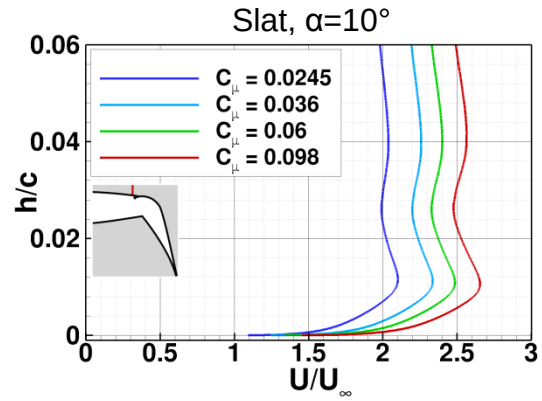

Stall behavior of a Coanda flap

Leading-edge device comparison

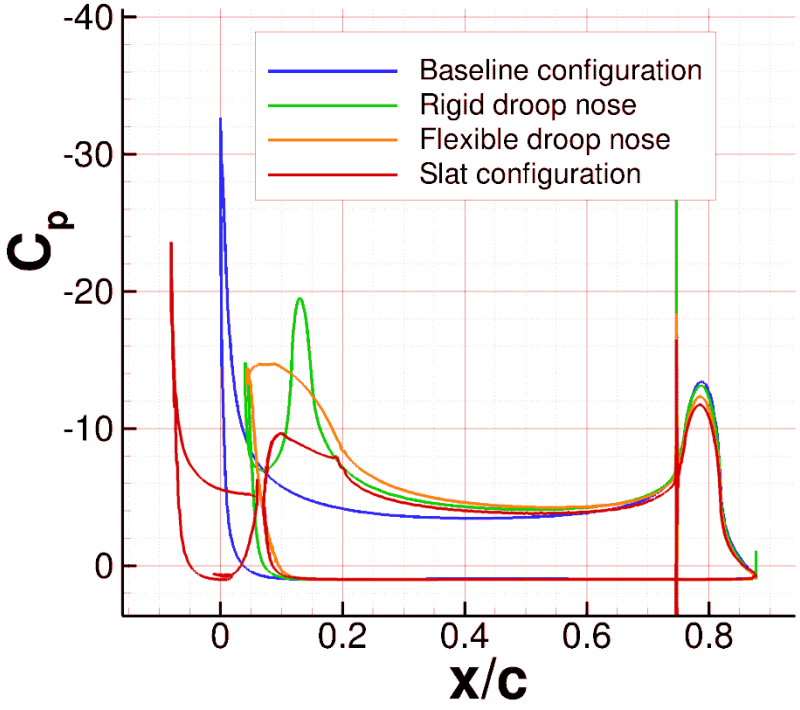

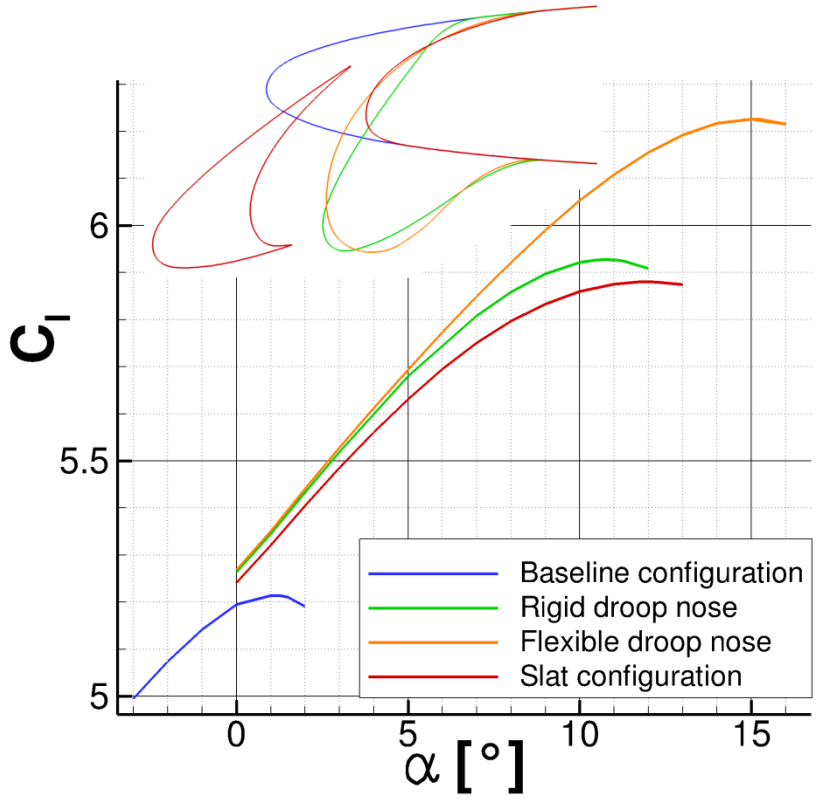

C_μ=0.06

Stall behavior of a Coanda flap

Leading-edge device comparison

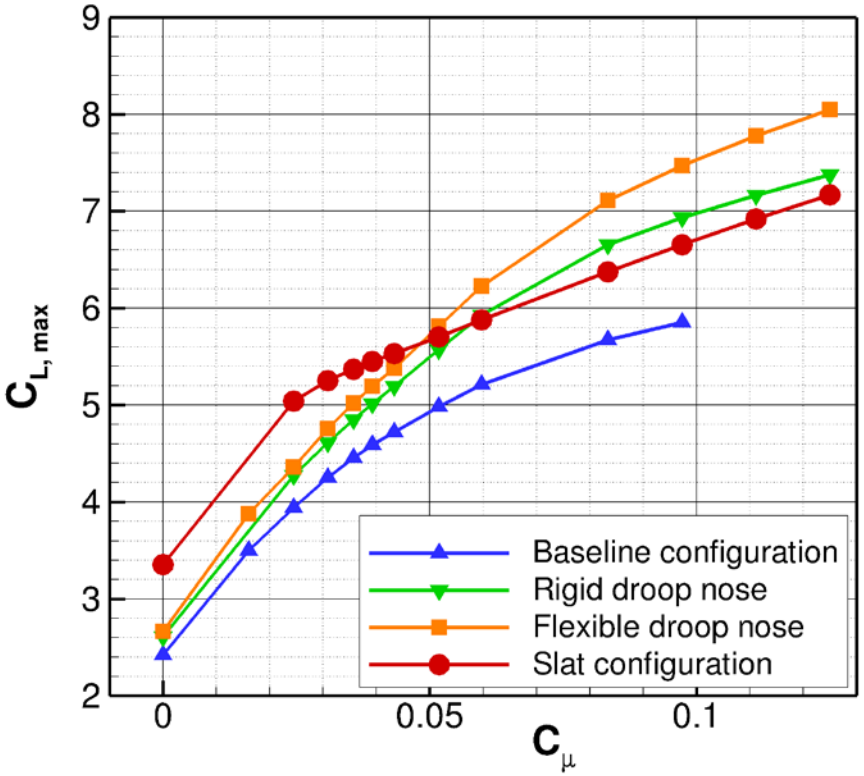

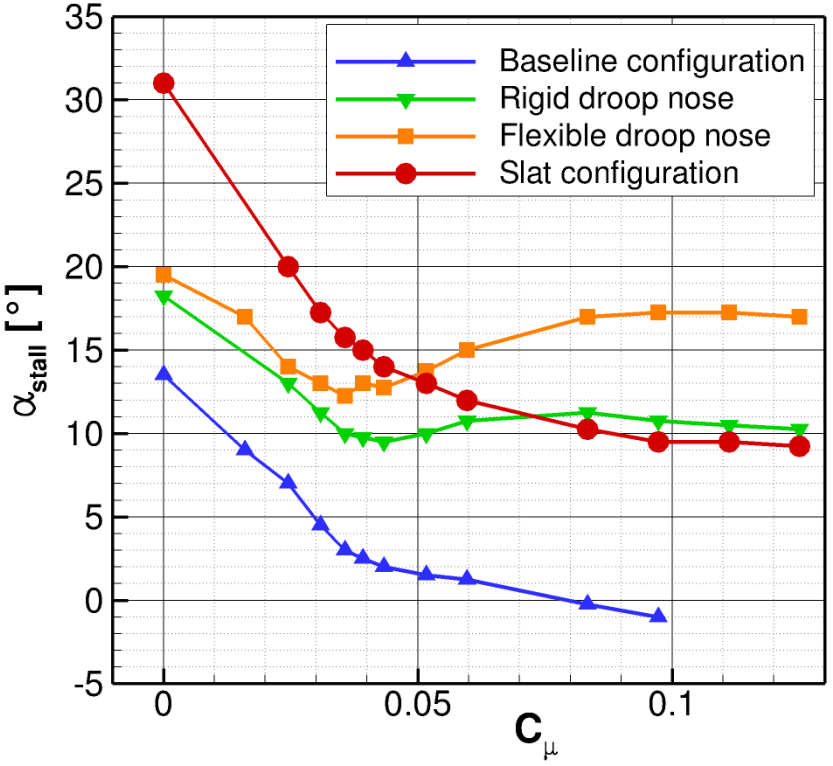

Thickness increase technique

$$f(x_{wingbox}) = 1$$

$$f'(x_{wingbox}) = 0$$

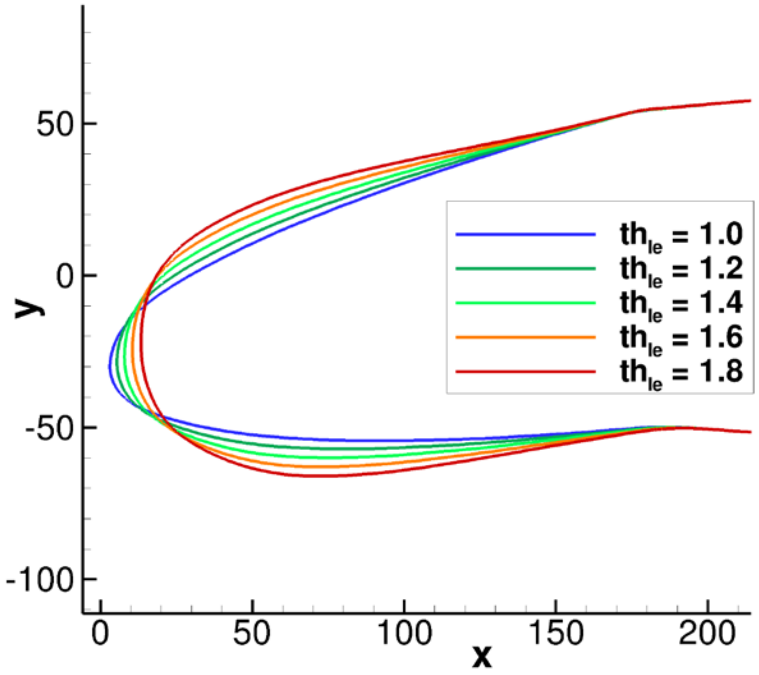

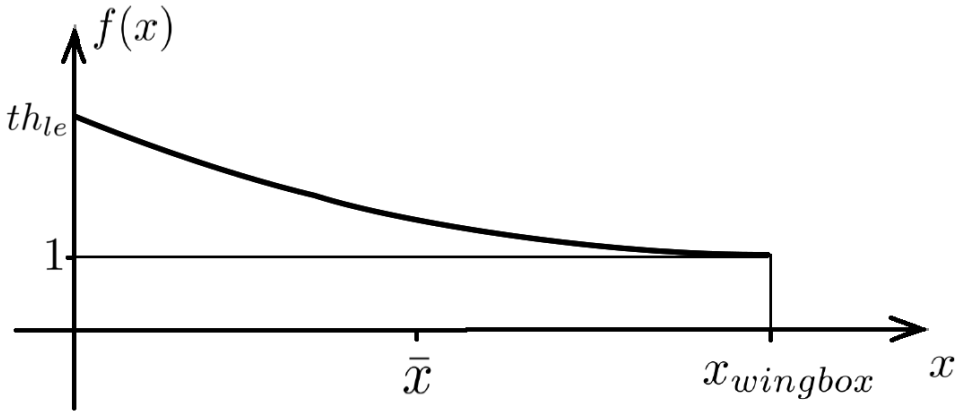

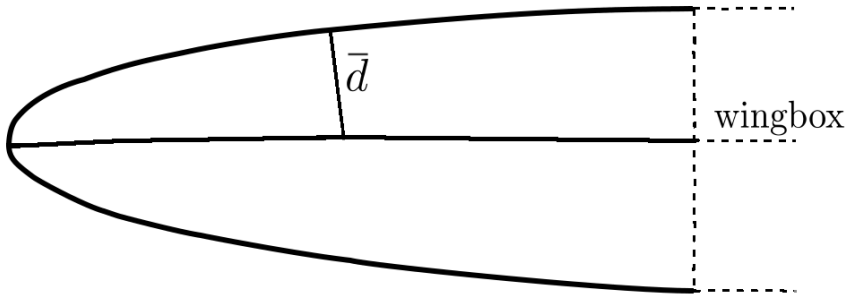

$$d_{new} = \bar{d} \cdot f(\bar{x})$$

3D Results

Alpha=6°: Overview

- Plenum pressure ratios adjusted for fully attached flow at α=6°
- Same plenum pressure ratios for Clean Nose and Droop Nose Config
  - ➢ Reduced O/B jet momentum for DN config

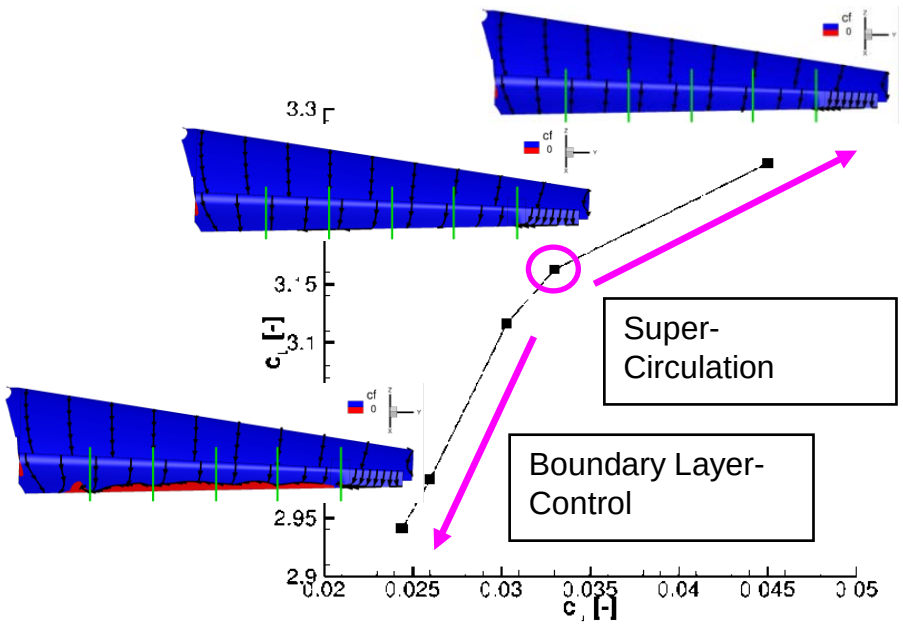

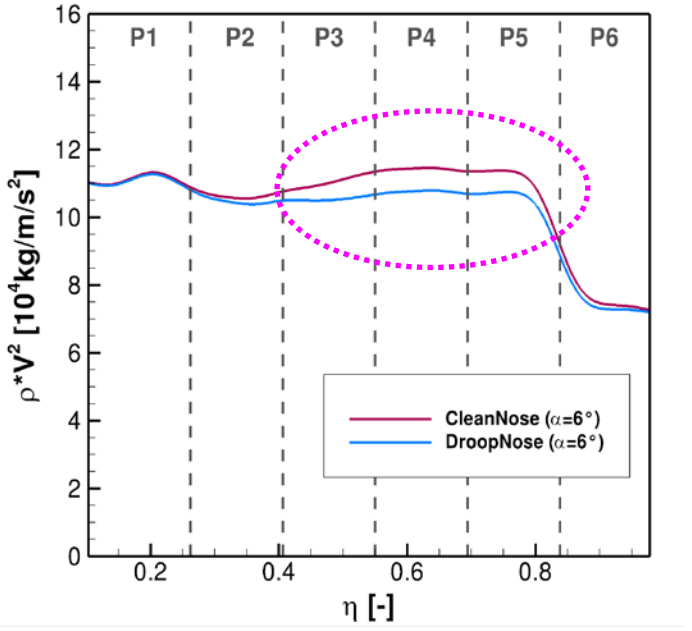

3D Analyses, smooth configuration

3D Geometry

- Aircraft geometry defined by a preliminary design study (PrADO)

  ⇒Realistic twist sweep and taper ratio

- Smooth implementation of the active high-lift devices to enable accurate meshing
- The wing is mounted at +3.44° w/r to the previous configuration

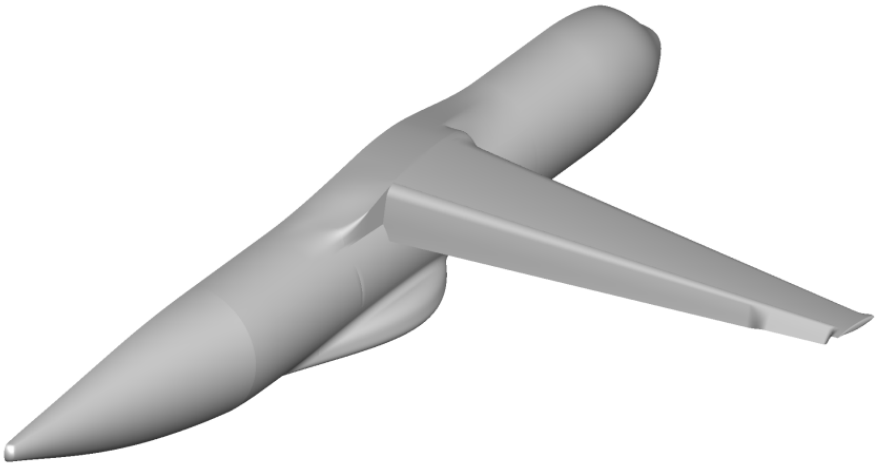

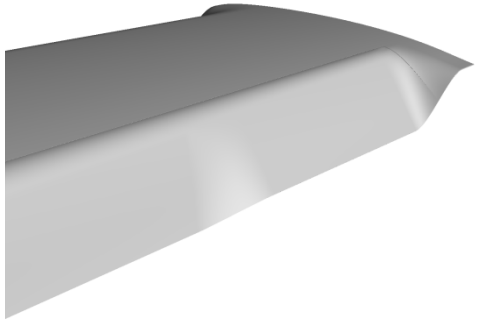

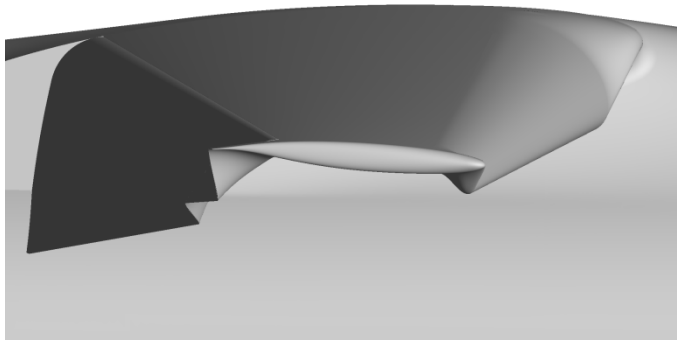

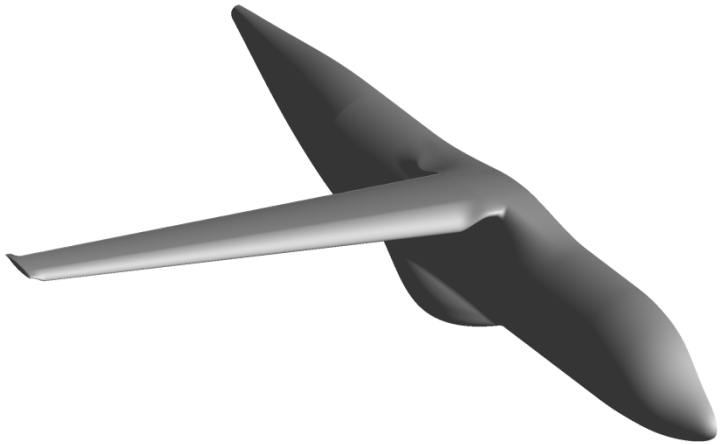

3D Analyses, structured mesh

3D Grid

- Structured layer on the surface
- Unstructured volume to farfield at 400 chords
- 5 unstructured shells to adapt the local point density
- 50 million points

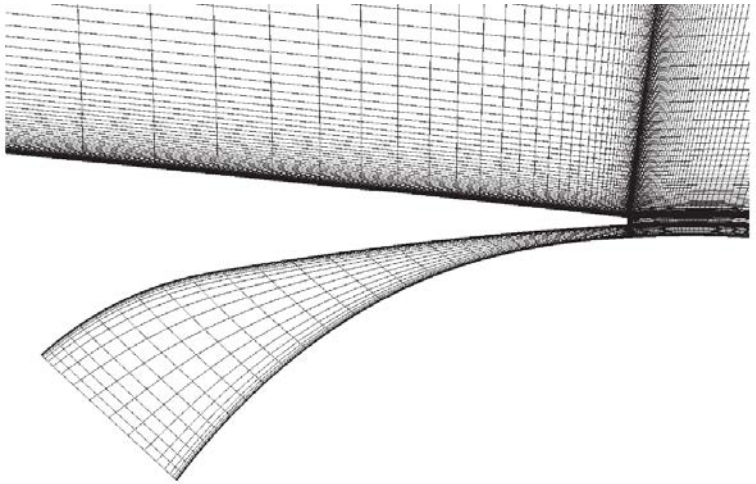

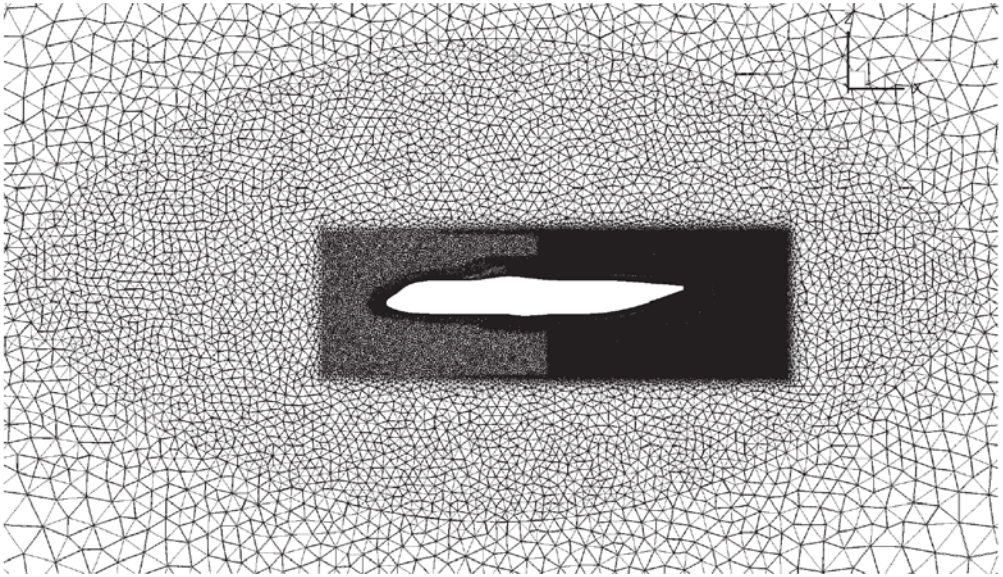

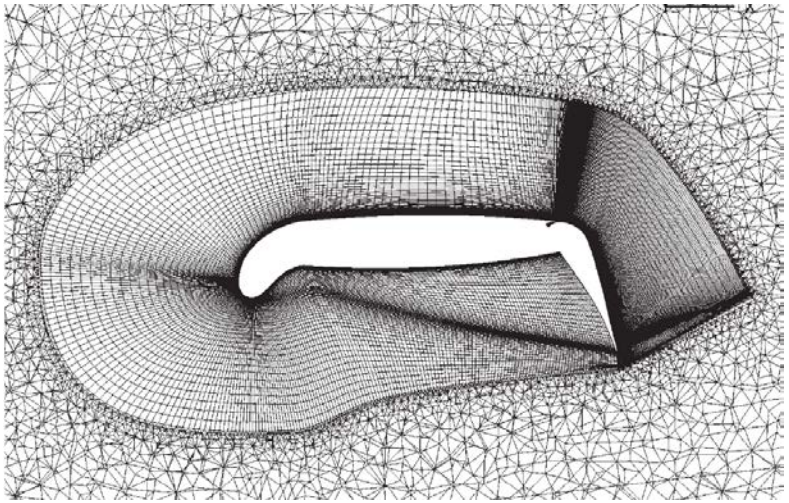

3D Analyses, structured mesh

3D Grid

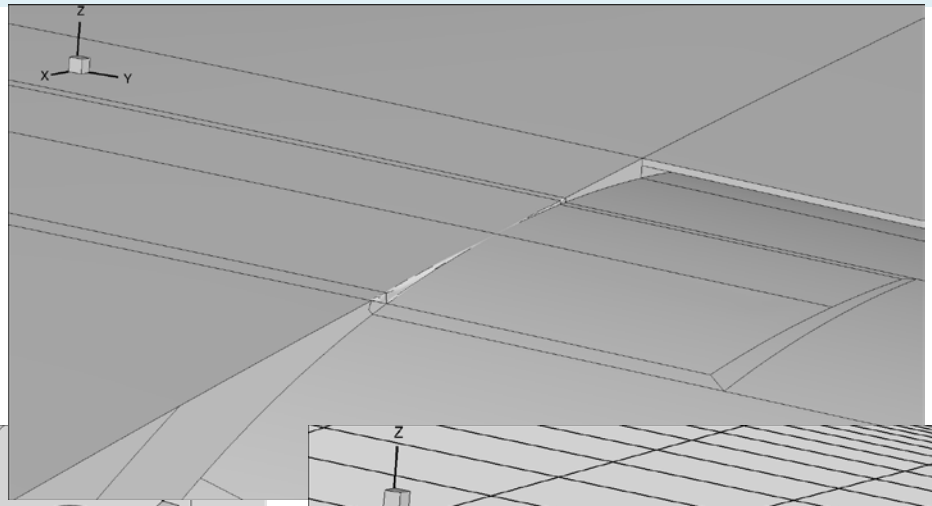

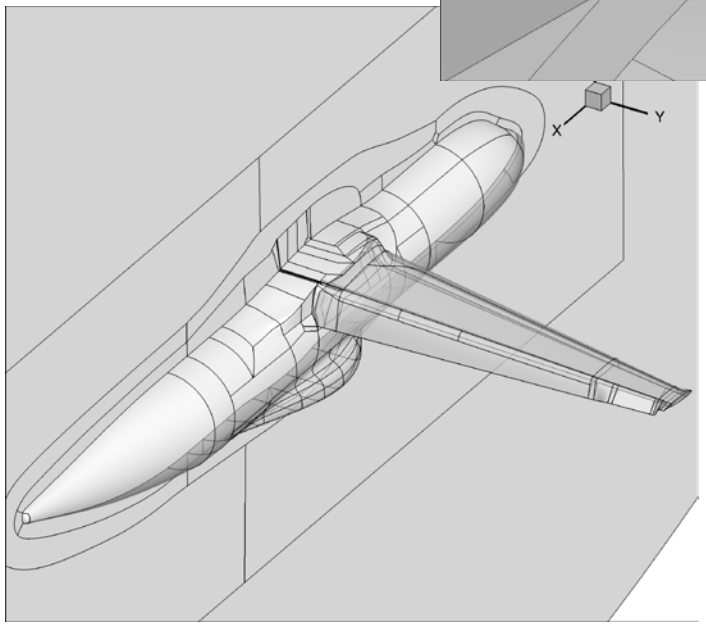

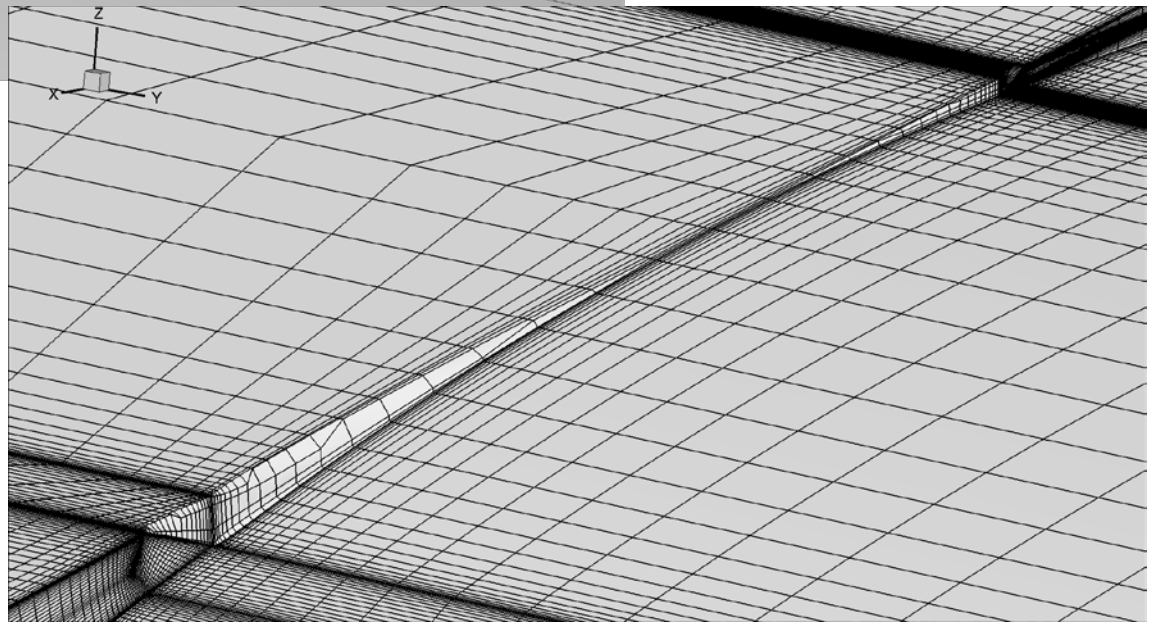

3D results, smooth configuration

Clean nose stall mechanism

- Reduction of circulation at η=0.65
- Trailing edge separation similar to 2D behavior
- Leading edge separation at η=0.65 (not observed in 2D)

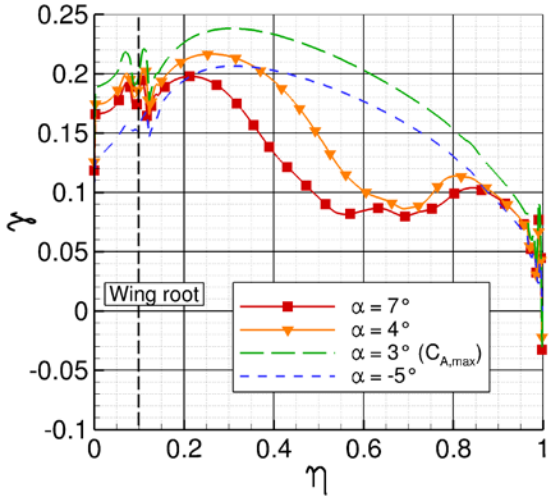

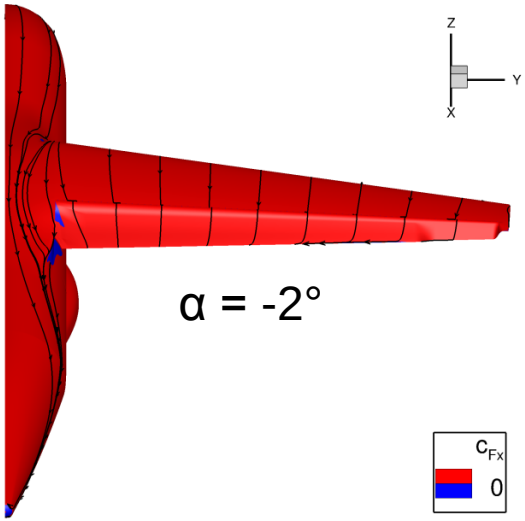

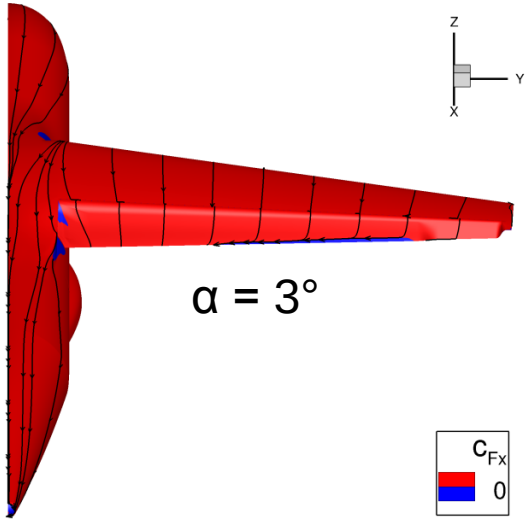

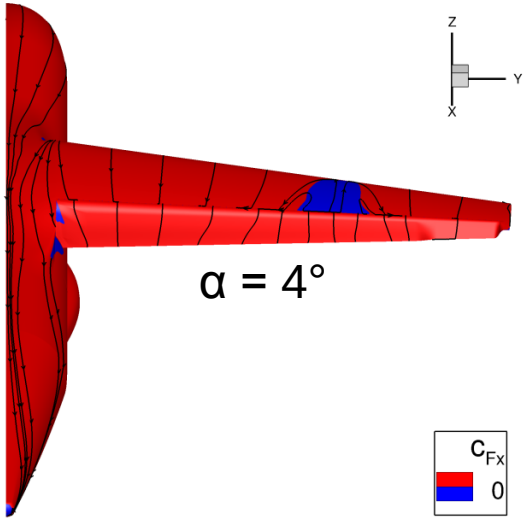

3D results, smooth configuration

Droop nose stall mechanism

- Reduction of circulation at wing root
- Trailing edge separation similar to 2D behavior
- Cross flow from the fuselage to the wing suction side

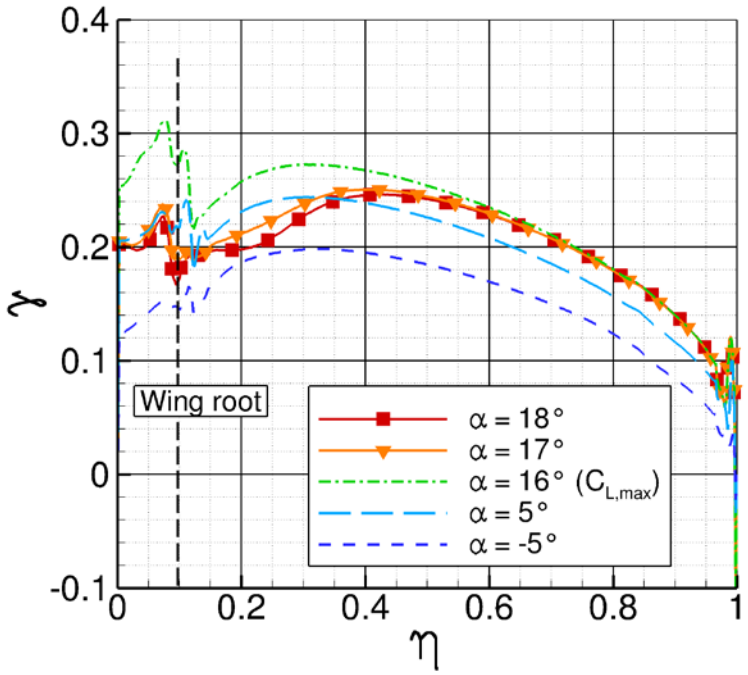

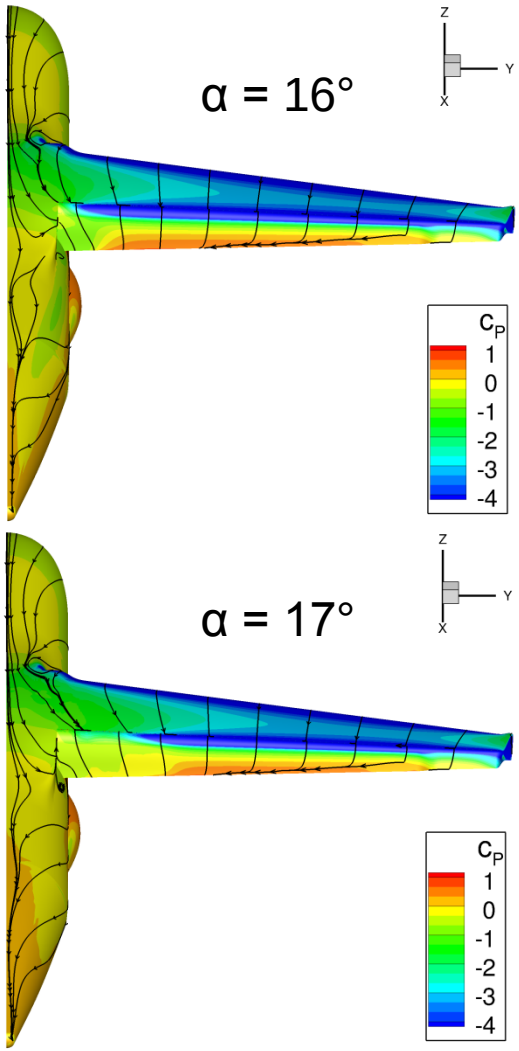

3D results, smooth configuration

3D lift curves

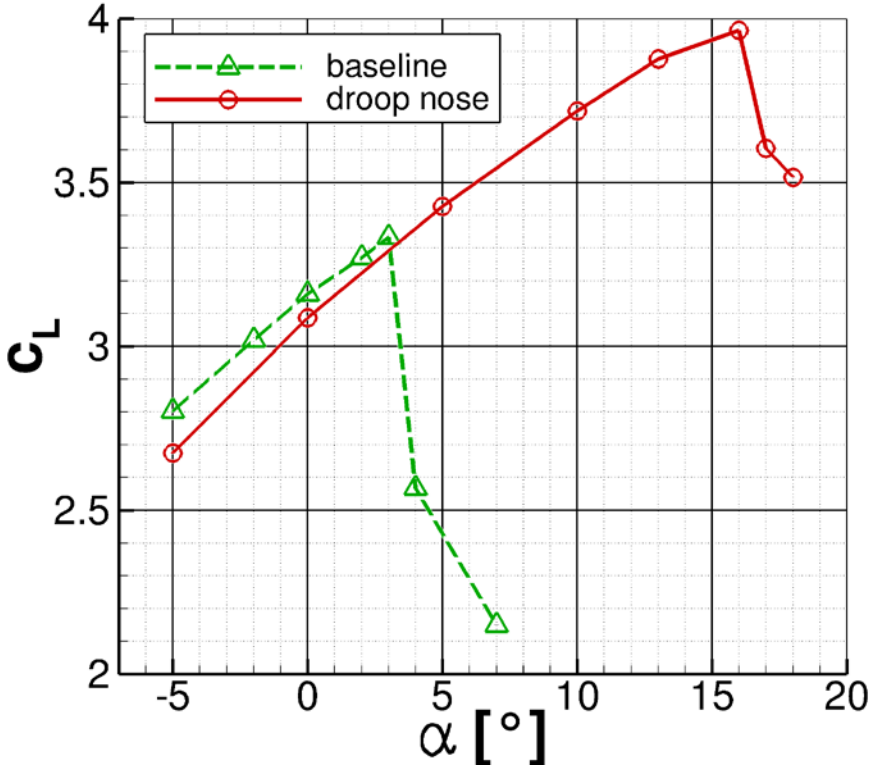

2D vs 3D (η=0.6, α_e by Prandtl)

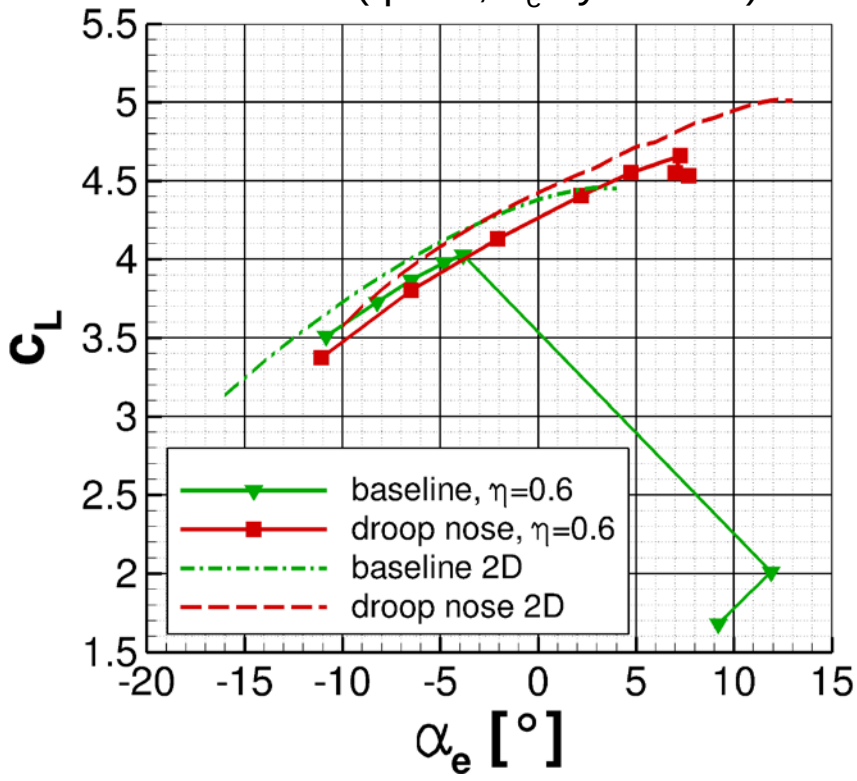

	2D	3D
Δc_L	+10.7%	+18.5%
$\Delta\alpha$	+7.0°	+13.0°

Overall lift performance

Different wing-root geometries at LE